Measurement of top quark polarisation in t-channel single top quark production

The CMS collaboration

E-mail: cms-publication-committee-chair@cern.ch

ABSTRACT: A first measurement of the top quark spin asymmetry, sensitive to the top quark polarisation, in t-channel single top quark production is presented. It is based on a sample of pp collisions at a centre-of-mass energy of $8\,\mathrm{TeV}$ corresponding to an integrated luminosity of $19.7\,\mathrm{fb}^{-1}$. A high-purity sample of t-channel single top quark events with an isolated muon is selected. Signal and background components are estimated using a fit to data. A differential cross section measurement, corrected for detector effects, of an angular observable sensitive to the top quark polarisation is performed. The differential distribution is used to extract a top quark spin asymmetry of $0.26\pm0.03(\mathrm{stat})\pm0.10(\mathrm{syst})$, which is compatible with a p-value of 4.6% with the standard model prediction of 0.44.

Contents

1 Introduction

The top quark is the heaviest elementary particle discovered so far. Its lifetime ($\approx 4 \times 10^{-25}$ s) is much shorter than the typical timescales of quantum chromodynamics (QCD). It is therefore the only quark that decays through electroweak interactions before hadronising. Furthermore, the parity-violating nature of the V-A electroweak interaction at the Wtb vertex means that only left-handed quarks are expected at this vertex. Thus, top quark decay products retain memory of the top quark spin orientation in their angular distributions. This fact turns the top quark into a powerful probe of the structure of the electroweak Wtb vertex.

In electroweak t-channel single top quark production, shown in figure 1, the standard model (SM) predicts that produced top quarks are highly polarised, as a consequence of the V-A coupling structure, along the direction of the momentum of the spectator quark
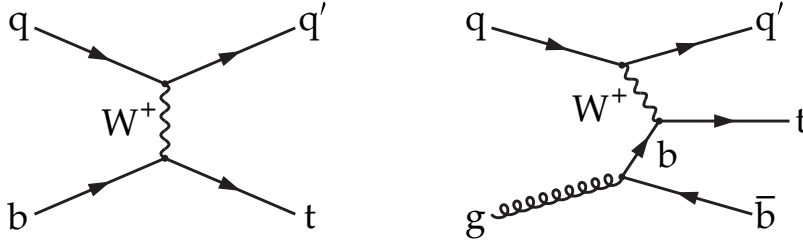
Figure 1. Feynman diagrams for single top quark production in the t-channel: (left) $(2) \rightarrow (2)$ and (right) $(2) \rightarrow (3)$ processes. Similar diagrams are expected for top antiquark production.

(q'), which recoils against the top quark [1, 2]. However, new physics models could also lead to a depolarisation in production by altering the coupling structure [3–6].

In this analysis, the top quark spin asymmetry

$$A_X \equiv \frac{1}{2} P_t \, \alpha_X = \frac{N(\uparrow) - N(\downarrow)}{N(\uparrow) + N(\downarrow)} \tag{1.1}$$

is used to probe the coupling structure, where P_t represents the top quark polarisation in production and α_X denotes the degree of the angular correlations of one of its decay products, denoted X (where for this analysis $X = \mu$), with respect to the spin of the top quark, the so-called spin-analysing power. The variables $N(\uparrow)$ and $N(\downarrow)$ are defined, for each top quark decay product from the decay chain $t \rightarrow bW \rightarrow b\mu\nu$, as the number of instances in which that decay product is aligned or antialigned, respectively, relative to the direction of the recoiling spectator quark momentum.

In this analysis, the muon is chosen as the top quark spin analyser because leptons have the highest spin-analysing power and since the muon identification efficiency is very high in the CMS detector. The spin-analysing power is exactly 1 at leading order (LO) in the SM. Its value can be modified by new physics that may be characterised by anomalous top quark coupling models arising from an effective extension of the coupling structure of the Wtb vertex [5].

The measurement of the top quark spin asymmetry, measured in t-channel single top quark events with one isolated muon in the final state, is the subject of this paper. The asymmetry is measured for top quark and antiquark events separately to be sensitive to potential CP-violation, which is predicted in some new physics models.

The analysis strategy is as follows: after applying an event selection designed to obtain a set of relatively high purity t-channel single top quark events, the signal and background composition of data is estimated using a binned likelihood fit. A top quark candidate is then reconstructed and the angle between the muon and the recoiling jet calculated in the top quark rest frame.

An unfolding technique is applied to obtain a differential cross section measurement of this angular distribution at parton level. From the unfolded distribution, the top quark spin asymmetry, which is directly related to the polarisation through eq. (1.1), is calculated for top quark and antiquark events, and their combination.

2   The CMS detector and event reconstruction

The central feature of the CMS apparatus is a superconducting solenoid of 6 m internal diameter, providing a magnetic field of 3.8 T. Within the solenoid volume are a silicon pixel and strip tracker, a lead tungstate crystal electromagnetic calorimeter (ECAL), and a brass and scintillator hadron calorimeter (HCAL), each composed of a barrel and two endcap sections. Muons are measured in gas-ionisation detectors embedded in the steel flux-return yoke outside the solenoid. Extensive forward calorimetry complements the coverage provided by the barrel and endcap detectors. A more detailed description of the CMS detector, together with a definition of the coordinate system used and the relevant kinematic variables, can be found in ref. [7].

The particle-flow algorithm [8, 9] reconstructs and identifies each individual particle in an event with an optimised combination of information from the various elements of the CMS detector. The energy of photons is directly obtained from the ECAL measurement. The energy of electrons is determined from a combination of the electron momentum at the primary interaction vertex, as determined by the tracker, the energy of the corresponding ECAL cluster, and the energy sum of all bremsstrahlung photons spatially compatible with originating from the electron track. The energy of muons is obtained from the curvature of the corresponding track. The energy of charged hadrons is determined from a combination of their momentum measured in the tracker and the matching ECAL and HCAL energy deposits, corrected for the response function of the calorimeters to hadronic showers. Finally, the energy of neutral hadrons is obtained from the corresponding corrected ECAL and HCAL energy. To mitigate the effect of pileup, i.e. additional proton-proton collisions whose signals in the detector sum to the products of the primary interaction that triggered the event, charged particles associated to non-leading primary vertices are vetoed.

The missing transverse momentum vector, $\vec{p}_T$, is defined as the projection onto the plane perpendicular to the beams of the negative vector sum of the momenta of all reconstructed particles in an event. Its magnitude is referred to as missing transverse energy (E_T).

3   Data and simulated samples

This study is based on the proton-proton collision data set recorded by the CMS detector at the CERN LHC in 2012 at a centre-of-mass energy 8 TeV, corresponding to an integrated luminosity of 19.7 ± 0.5 fb^{-1} [10].

Single top quark t-channel events from Monte Carlo (MC) simulation are generated with the next-to-leading-order (NLO) MC generator POWHEG 1.0 [11–13], interfaced with PYTHIA 6.4 [14] for the parton showering, in which τ lepton decays are modelled with TAUOLA [15]. The 5-flavour scheme (5FS) is used in the generation, i.e. inherent b quarks are considered among the incoming particles as in figure 1 (left). As an alternative NLO generator, used to assess the dependence of the analysis on the modelling of signal, we use aMC@NLO 2.1.2 [16] interfaced with PYTHIA 8.180 [17], with the 4-flavour scheme (4FS), i.e. b quarks in the initial state are only produced via gluon splitting as in figure 1 (right). The measured results are compared with predictions from the aforementioned NLO generators

and the LO generator COMPHEP 4.5 [18], interfaced with PYTHIA 6, with a matching procedure between LO 5FS and 4FS diagrams based on the transverse momentum p_T of the associated b quark [19]. Special samples are generated using COMPHEP 4.5 including a Wtb coupling with anomalous structure.

Several SM processes are taken into account as backgrounds in the analysis. The POWHEG 1.0 generator interfaced with PYTHIA 6 is also used to model the W-associated (tW) and s-channel single top quark background events. The $t\bar{t}$, W boson in association with jets (W+jets), and Drell-Yan in association with jets (Z/γ^*+jets) processes are generated with MADGRAPH 5.1 [20] interfaced with PYTHIA 6. TAUOLA is used to simulate τ lepton decays. Up to three (four) additional partons are generated at matrix-element (ME) level in $t\bar{t}$ (W+jets and Z/γ^*+jets) events. A procedure, implemented during event generation, based on the so-called "MLM prescription" [21, 22], avoids double counting jets generated simultaneously by the ME and by the parton shower (PS) simulations. An alternative sample of W+jets generated with SHERPA 1.4.0 at NLO [23, 24] is used to compare the modelling of this background. Diboson production (WW, WZ, ZZ) is simulated using PYTHIA 6. Multijet events (i.e. events with the muon not originating from a leptonically decaying W or Z boson) are modelled using statistically independent samples in data, as detailed in section 6.1. Other special samples of signal and background are generated with different values for generator parameters (e.g. top quark mass, renormalisation and factorisation scales, etc.), and used to estimate the corresponding systematic uncertainties.

All single top quark processes are normalised to approximate next-to-next-to-leading-order (NNLO) predictions [25] ($\sigma_{t\text{-channel}} = 87.1\,\text{pb}$, $\sigma_{s\text{-channel}} = 5.55\,\text{pb}$, $\sigma_{\text{tW}} = 22.2\,\text{pb}$). Top quark pair production is normalised to a complete NNLO prediction in QCD that includes soft gluon resummation to next-to-next-to-leading-log order, as calculated with the TOP++2.0 program [26] ($\sigma_{t\bar{t}} = 252.9\,\text{pb}$). The W+jets and Z/γ^*+jets production cross sections times branching fraction are calculated at NNLO with FEWZ [27] ($\sigma_{\text{W+jets}}\,\mathcal{B}(\text{W} \to \ell\nu) = 37\,509\,\text{pb}$, and $\sigma_{Z/\gamma^*\text{+jets}}\,\mathcal{B}(Z/\gamma^* \to \ell^+\ell^-) = 3504\,\text{pb}$ at a generator-level threshold of $m_{\ell^+\ell^-} > 50\,\text{GeV}$, where $\ell = \text{e}$, μ, or τ). The diboson cross sections are calculated at NLO with MCFM 5.8 [28] ($\sigma_{\text{WW}} = 54.8\,\text{pb}$, $\sigma_{\text{WZ}} = 33.2\,\text{pb}$, and $\sigma_{\text{ZZ}} = 8.1\,\text{pb}$).

The effect of pileup is evaluated using a simulated sample of minimum-bias events produced using PYTHIA 6, superimposed onto the events in the simulated samples described above, taking into account in-time and out-of-time pileup contributions. The events are then reweighted to reproduce the true pileup distribution inferred from the data. The procedure is validated by comparing the number of observed primary vertices between data and simulation.

All generated events undergo a full GEANT4 [29] simulation of the detector response.

4 Event selection

The study presented here focuses on the $t \to bW \to b\mu\nu$ decay channel. Signal events are characterised by exactly one isolated muon, large $\not{E}_T$ (originating from the neutrino in the leptonic decay of the W boson), one central b jet from the top quark decay, and an additional untagged jet (j$'$) from the spectator quark (q$'$) from the hard-scattering

process, which is preferentially produced in the forward region of the detector. A second b jet produced in association with the top quark can also be present in the detector, although it yields a softer p_T spectrum relative to the b jet from the top quark decay. The event selection applied in the measurement of the production cross section in the same channel [30] is closely followed.

Trigger selection is based on the presence of at least one isolated muon with $p_T >$ 24 GeV and $|\eta| < 2.1$.

One isolated muon candidate is required to originate from the leading primary vertex, which is defined as the vertex with the largest value of the summed p_T^2 of its associated charged tracks. Muon candidates are accepted if they pass the following requirements: p_T of at least 26 GeV, $|\eta| < 2.1$, quality and identification criteria optimised for the selection of prompt muons, and a relative isolation requirement of $I_{rel} < 0.12$. The relative isolation, I_{rel}, is defined by the scalar sum, divided by the p_T of the muon, of the transverse energies deposited by stable charged hadrons, photons, and neutral hadrons where deposits linked to pileup are subtracted within a cone of radius $\Delta R = \sqrt{(\Delta\eta)^2 + (\Delta\phi)^2} = 0.4$ (where ϕ is the azimuthal angle in radians) around the muon direction. Events are rejected if an additional muon or electron candidate is present. The selection requirements for these additional electrons/muons are as follows: looser identification and isolation criteria, $p_T >$ 10 (20) GeV for muons (electrons), and $|\eta| < 2.5$.

Jets are reconstructed from the particle-flow candidates and clustered with the anti-k_T algorithm [31, 32] with a distance parameter of 0.5. The influence of pileup is mitigated using the charged hadron subtraction technique [33]. The jet momentum is determined as the vectorial sum of all particle momenta in the jet. An offset correction is applied to the transverse jet momenta to account for contributions from pileup. Further corrections are applied to account for the non-flat detector response in η and p_T of the jets. The corrected jet momentum is found from simulation to be within 5% to 10% of the true momentum over the whole p_T spectrum and detector acceptance. The corrections are propagated to the measured $\vec{p}_T$ as it depends on the corrected jets through the clustered tracks. Additional selection criteria are applied to each event to remove spurious jet-like features originating from isolated noise patterns in certain HCAL regions. The analysis considers jets within $|\eta| < 4.5$ whose calibrated transverse energy is greater than 40 GeV . The event is accepted for further analysis only if at least two such jets are present.

To reduce the large background from W+jets events, a b tagging algorithm based on combined information from secondary vertices and track-based lifetimes [34, 35] is used. A tight selection is applied on the b tagging discriminant, which corresponds to an efficiency of $\approx$50% for jets originating from true b quarks and a mistagging rate of $\approx$0.1% for other jets in the signal simulation. The b tagging performance in simulation is corrected to better match the performance observed in data [35], using scale factors that depend on the p_T and η of the selected jets.

Corrections are applied to the simulation, where necessary, to account for known differences relative to data. Single-muon trigger efficiencies and lepton reconstruction and identification efficiencies are estimated with a "tag-and-probe" method [36, 37] from Z/γ^*+jets data. B tagging and misidentification efficiencies are estimated by dedicated analyses per-

formed with statistically independent selections [35]. A smearing of the jet momenta is applied to account for the known difference in jet energy resolution (JER) in simulation compared to data [38]. The effects of all these corrections are found to be small.

To classify signal and control regions, different event categories, denoted "Njets Mtag(s)" are defined, where N is the total number of selected jets (2 or 3) and M is the number of those jets passing additionally the b tagging requirements (0, 1, or 2). The "2jets 1tag" category defines the region used for signal extraction, whereas the other categories, enriched in background processes with different compositions, are used for the control samples discussed in section 6. The "2jets 1tag" category is separated into a control region and a signal region, depending on the value of a multivariate discriminant, described below.

In the "2jets 1tag" category, a top quark candidate is reconstructed from the b jet, the muon, and a neutrino candidate. A neutrino candidate is constructed as described in ref. [39]. The neutrino p_z^ν momentum is found by requiring a W boson mass constraint from momentum conservation using the muon and missing transverse momenta. In the other categories, the jet with the highest value of the b tagging discriminant is used for top quark reconstruction.

Multijet events are suppressed by setting a threshold on the output of a dedicated boosted decision tree ($\mathrm{BDT_{multijet}}$), trained using the following input variables:

- the missing transverse energy, $\not{E}_\mathrm{T}$;

- the invariant mass of the top quark candidate, $m_{\mathrm{b\mu\nu}}$;

- the transverse mass of the W boson candidate,
$m_\mathrm{T}(W) = \sqrt{\left(p_\mathrm{T}^\mu + \not{E}_\mathrm{T}\right)^2 - \left(p_x^\mu + \vec{\not{p}}_{\mathrm{T},x}\right)^2 - \left(p_y^\mu + \vec{\not{p}}_{\mathrm{T},y}\right)^2}$;

- the transverse momentum of the untagged jet, $p_\mathrm{T}^{\mathrm{j}'}$;

- the event isotropy, defined as $(\mathcal{S}_\mathrm{max} - \mathcal{S}_\mathrm{min})/\mathcal{S}_\mathrm{max}$ with $\mathcal{S} \equiv \sum_i^{\mu,\mathrm{jets}} |\vec{n} \cdot \vec{p}_i|$, where the unit vector in the transverse r–ϕ plane, $\vec{n} = (\cos\phi, \sin\phi)$, can be chosen to either maximise or minimise $\mathcal{S}$.

To reject background events, a second boosted decision tree, $\mathrm{BDT_{W/t\bar{t}}}$, is used to separate signal from $t\bar{t}$ and W+jets events. Training is performed with the following input observables:

- the invariant mass of the top quark candidate, $m_{\mathrm{b\mu\nu}}$;

- the absolute pseudorapidity of the untagged jet, $|\eta_{\mathrm{j}'}|$;

- the absolute pseudorapidity of the b-tagged jet, $|\eta_\mathrm{b}|$;

- the invariant mass of the b-tagged jet from the summed momenta of the clustered tracks, m_b;
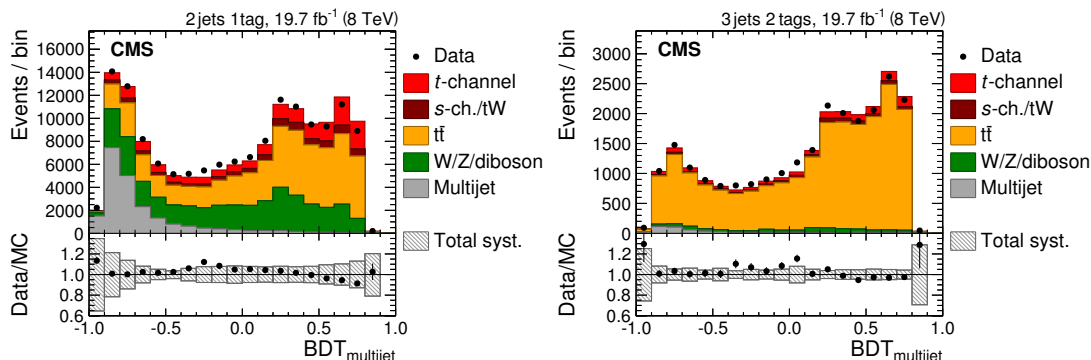
Figure 2. Distributions of the $BDT_{multijet}$ discriminant in the (left) "2jets 1tag" and (right) "3jets 2tags" categories. The predictions are normalised to the results of the fit described in section 7. The bottom panels in both plots show the ratio between observed and predicted event counts, with a shaded area to indicate the systematic uncertainties affecting the background prediction and vertical bars indicating statistical uncertainties.

- the transverse momentum of the muon, p_T^μ;

- the transverse momentum of the b-tagged jet, p_T^b;

- the transverse mass of the W boson candidate;

- the missing transverse energy, $\not{E}_T$;

- the total invariant mass of the top quark candidate and the untagged jet system, $\hat{s}$;

- the transverse momentum of the hadronic final-state system, $H_T = (\vec{p}_b + \vec{p}_{j'})_T$.

By construction, the BDT discriminant ranges between $+1$ and -1, with the algorithm trained such that the resulting distribution peaks at a high BDT discriminant value for signal-like events and at a low value for background-like events. The distribution of the $BDT_{multijet}$ discriminant is shown in figure 2 in two categories, with the multijet events shape and normalisation extracted as described in section 6.1. To reject multijet events, we only use events that pass the threshold $BDT_{multijet}$ discriminant > -0.15 in the analysis. Figure 3 shows the distribution of the $BDT_{W/t\bar{t}}$ discriminant in the "2jets 1tag" and "3jets 2tags" categories after applying the selection requirement on the $BDT_{multijet}$ discriminant.

Figure 4 shows the distributions of the $|\eta_{j'}|$ and $m_{b\mu\nu}$ variables in the "2jets 1tag" category. These variables have the highest ranking in the decision of the $BDT_{W/t\bar{t}}$.

To select a signal-enhanced phase space, an additional selection is imposed on the $BDT_{W/t\bar{t}}$ discriminant. The optimal working point is found to be $BDT_{W/t\bar{t}}$ discriminant > 0.45 by studying the analysis sensitivity with pseudo-data from simulated events.

All BDT input variables are found to be well modelled by the MC simulation. The BDTs are trained and tested on statistically independent samples, with no overtraining observed.
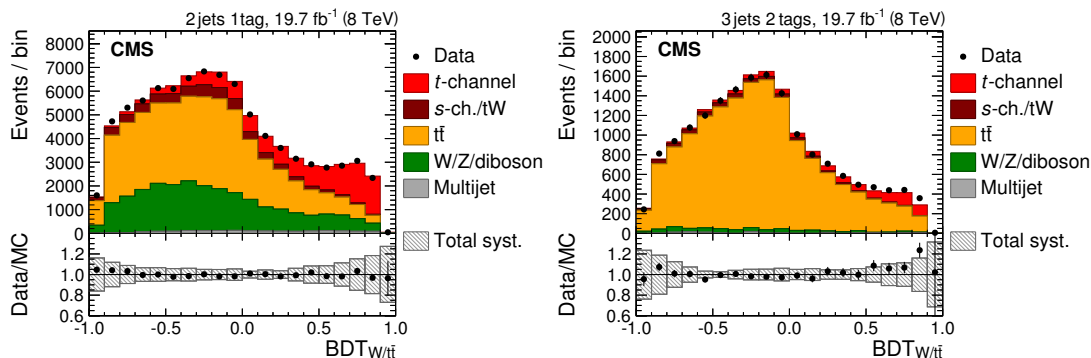
Figure 3. Distributions of the $\mathrm{BDT}_{\mathrm{W/t\bar{t}}}$ discriminant in the (left) "2jets 1tag" and (right) "3jets 2tags" categories. The predictions are normalised to the results of the fit described in section 7. The bottom panels in both plots show the ratio between observed and predicted event counts, with a shaded area to indicate the systematic uncertainties affecting the background prediction and vertical bars indicating statistical uncertainties.
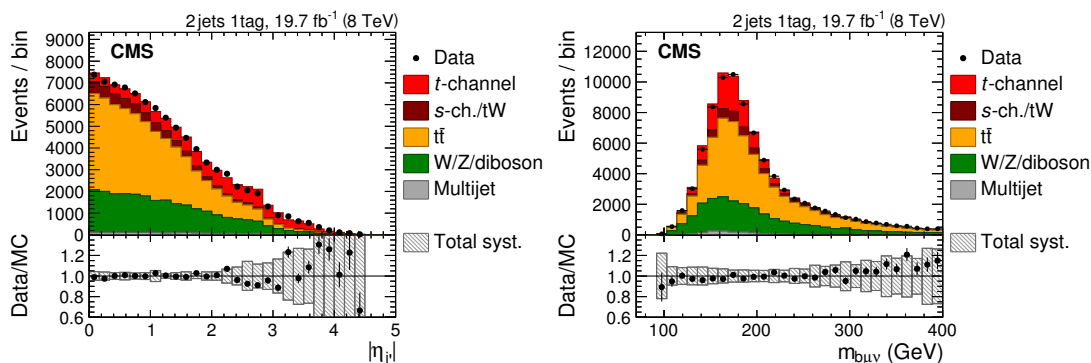
Figure 4. Distributions of the $|\eta_{\mathrm{j'}}|$ (left) and $m_{\mathrm{b\mu\nu}}$ (right) variables in the "2jets 1tag" category. In both plots, the rejection of multijet events is performed by requiring $\mathrm{BDT}_{\mathrm{multijet}} > -0.15$. The predictions are normalised to the results of the fit described in section 7. The bottom panels in both plots show the ratio between observed and predicted event counts, with a shaded area to indicate the systematic uncertainties affecting the background prediction and vertical bars indicating statistical uncertainties.

5 The $\cos\theta_\mu^*$ distribution of top quark decay products

The angle between a top quark decay product X (W, ℓ, ν, or b) and an arbitrary polarisation axis $\vec{s}$ in the top quark rest frame, θ_X^*, is distributed according to the following differential cross section:

$$\frac{1}{\sigma}\frac{\mathrm{d}\sigma}{\mathrm{d}\cos\theta_X^*} = \frac{1}{2}(1 + P_{\mathrm{t}}^{(\vec{s})}\alpha_X\cos\theta_X^*) = \left(\frac{1}{2} + A_X\cos\theta_X^*\right). \tag{5.1}$$

The variable $P_{\mathrm{t}}^{(\vec{s})}$ denotes the single top quark polarisation along the chosen axis, and α_X the spin-analysing power as defined in section 1. In the SM, the top quark spin tends to be aligned with the direction of the spectator quark momentum, resulting in a high degree of polarisation. Hence, an excess of events where the spectator quark momentum is antialigned with the top quark spin would clearly indicate an anomalous coupling structure.
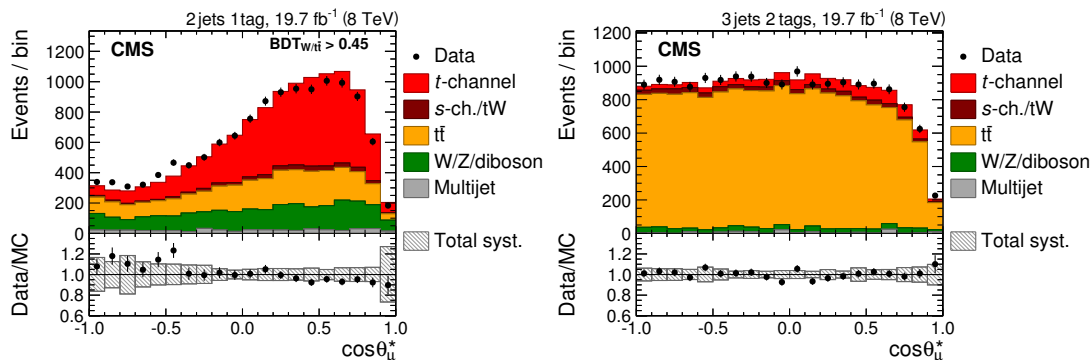
Figure 5. Distributions of $\cos\theta_\mu^*$ in the (left) signal region defined by $\mathrm{BDT_{W/t\bar{t}}} > 0.45$ in the "2jets 1tag" category and (right) "3jets 2tags" control region. In both plots, the rejection of multijet events is performed by requiring $\mathrm{BDT_{multijet}} > -0.15$. The predictions are normalised to the results of the fit described in section 7. The bottom panels in both plots show the ratio between observed and predicted event counts, with a shaded area to indicate the systematic uncertainties affecting the background prediction, and vertical bars indicating statistical uncertainties.

Single top quark polarisation is studied in the t-channel process through the angular asymmetry A_μ of the muon, with the polarisation axis defined as pointing along the untagged jet (j′) direction in the top quark rest frame.

Figure 5 shows the reconstructed distribution of $\cos\theta_\mu^*$ in the "2jets 1tag" (for $\mathrm{BDT_{W/t\bar{t}}} > 0.45$) and "3jets 2tags" categories. The observed distribution is expected to differ from the parton-level prediction because of detector effects and the kinematic selection applied, with the most significant effect being the relatively small number of selected events close to $\cos\theta_\mu^* = 1$. An overall trend in the ratio between data and simulation is observed that suggests a slightly less asymmetric shape than predicted by the SM.

In this analysis, a χ^2-fit is performed of the unfolded $\cos\theta_\mu^*$ differential cross section to estimate A_μ based on eq. (5.1).

6 Studies of background modeling

Statistically independent control samples are used for several purposes in this analysis. Samples in which the isolation requirement on the muon is inverted are used to extract templates for estimating the contamination by multijet events, while samples with different jet and b-tagged jet multiplicities are used to validate the simulation of W+jets and $t\bar{t}$ events, or to provide additional constraints on the in situ determination of background and signal strengths relative to the SM.

6.1 Estimation of multijet events background

The yield of the multijet events background in the different categories is measured by performing fits to the $\mathrm{BDT_{multijet}}$ discriminant distributions for each "Njet Mtag" category where a significant contamination from this process is expected. A binned maximum-likelihood (ML) fit to the data is performed using two components: multijet events (unconstrained) and the sum of all other processes (constrained to be within $\pm20\%$ of the

expected yield using a log-normal prior that the fit constrains further). The latter category includes the signal. A normalised distribution (template) for the sum of other processes is taken from simulation. The multijet events template is obtained from a statistically independent multijet-enriched data sample with an inverted isolation requirement, as defined above. It is verified that the $\mathrm{BDT}_{\mathrm{multijet}}$ discriminant distributions for multijet events are not significantly affected by this altered event selection.

Uncertainties on the multijet events yields are estimated conservatively to be $\pm 50\%$. In addition, an uncertainty on the shape is taken into account by using a modified inverted isolation requirement. Together, these are used to estimate the systematic uncertainty associated with this procedure, as discussed in section 9.

6.2 W+jets model validation and correction

After estimating the multijet events contribution to the signal region, the agreement between the expectations and the data is verified in several control regions for all the $\mathrm{BDT}_{\mathrm{W}/t\bar{t}}$ inputs, for the $\mathrm{BDT}_{\mathrm{W}/t\bar{t}}$ response, for $\cos\theta_{\mu}^{*}$, and for a number of additional variables. Among all the control regions considered, $\cos\theta_{\mu}^{*}$ and p_{T} of the reconstructed W boson are observed to be mismodelled in the "2jets 0tags" control region; this region is expected to be enriched in W+jets events.

A similar disagreement between data and the MADGRAPH prediction in the $\cos\theta_{\mu}^{*}$ distribution is observed in data collected at $\sqrt{s} = 7\,\mathrm{TeV}$ in the context of a different analysis [30]. Investigations using different MC generators and their associated settings show that SHERPA [40] provides a better description of $\cos\theta_{\mu}^{*}$ in this control region at both centre-of-mass energies.

Although this control region is not used in the fit, additional investigations have been performed to check whether this mismodelling can potentially affect the signal region. The MADGRAPH and SHERPA samples are found to differ mostly in the $\cos\theta_{\mu}^{*}$ distribution for events with a W boson produced in association with jets from gluon fragmentation, which constitutes a major component of the "2jets 0tags" region, but is a very small fraction of the "2jets 1tag" signal region.

In the kinematic region studied by this analysis, MADGRAPH reproduces the W+jets kinematic distributions better than SHERPA. Moreover, for computational reasons, the approximation of using b and c quarks as massless in the generation of the SHERPA samples causes the relative fraction of heavy quarks to be unrealistically large. For these reasons, MADGRAPH is chosen as the default generator in this analysis, and a reweighting of the W+jets events simulated with MADGRAPH is performed in all signal and control regions using the event ratio between the two generators as a function of $\cos\theta_{\mu}^{*}$, separately for each flavour component, in the "2jets 0tags" control region.

6.3 $t\bar{t}$ model validation

To validate the modelling of $t\bar{t}$ events, we compare simulated events to data in the "3jets 2tags" control region for the most relevant observables. In particular, figures 2 (right), 3 (right), and 5 (right) show the $\mathrm{BDT}_{\mathrm{multijet}}$ and $\mathrm{BDT}_{\mathrm{W}/t\bar{t}}$ discriminants,

and the $\cos\theta_\mu^*$ distribution, respectively. This control region is also used in the fit described in section 7.

The MADGRAPH model of $t\bar{t}$ production is known to predict a harder top quark p_T (p_T^t) spectrum than observed in data [41, 42]. The spectrum of generator-level top quarks in $t\bar{t}$ events is therefore reweighted so that it reproduces the measured differential cross section as a function of p_T^t.

In conclusion, the $t\bar{t}$ modelling provided by MADGRAPH after applying the p_T^t reweighting is found to be in reasonable agreement with data.

7 Extraction of signal and background yields

The signal and background components are estimated by means of a simultaneous ML fit to the distribution of the $\text{BDT}_{W/t\bar{t}}$ discriminant in the "2jets 1tag" and "3jets 2tags" regions. The inclusion of the $t\bar{t}$-dominated "3jets 2tags" region in the fit provides an additional constraint on the $t\bar{t}$ background. This also reduces correlations of the estimated $t\bar{t}$ yield with other contributions.

For all background processes, except the multijet events background, templates from the MC samples are used. The multijet events template is obtained from data by inverting the isolation selection, as discussed previously, and its normalisation is kept fixed to the estimated yield described in section 6.1. To reduce the number of free parameters, several processes that have a similar distribution in both $\cos\theta_\mu^*$ and the $\text{BDT}_{W/t\bar{t}}$ discriminant are merged into a single contribution:

- Signal: t-channel single top quark production, treated as unconstrained.

- Top quark background: $t\bar{t}$, s-channel and tW single top quark production, with their relative fractions taken from simulation; a constraint of $\pm 20\%$ using a log-normal prior is applied.

- W/Z/diboson: W+jets, Z/γ^*+jets, and diboson production, with their relative fractions taken from simulation, have a constraint of $\pm 50\%$ using a log-normal prior.

The results of the three fits, and the post-fit uncertainties for top quark events, top antiquark events, and their combination, are presented in table 1 as scale factors to be applied to simulation yields, while table 2 shows the number of events exceeding the threshold on the $\text{BDT}_{W/t\bar{t}}$ discriminant >0.45. The number of top quark events is greater than the number of top antiquark events due to the up-quark density being larger than either the down-quark or up-antiquark densities at large values of Bjorken x in the incoming protons.

8 Unfolding

An unfolding procedure is used to determine the differential cross section as a function of $\cos\theta_\mu^*$ at the parton level. It accounts for distortions from detector acceptance, selection efficiencies, imperfect reconstruction of the top quark candidate, and the approximation made in treating the direction of the untagged jet as the spectator quark direction.

Processes	t	$\bar{\text{t}}$	$\text{t} + \bar{\text{t}}$
Signal	1.10 ± 0.03	1.20 ± 0.05	1.13 ± 0.03
Top quark bkg.	1.06 ± 0.02	1.08 ± 0.02	1.07 ± 0.01
W/Z/diboson	1.26 ± 0.05	1.21 ± 0.06	1.24 ± 0.04

Table 1. Estimated scale factors and uncertainties from the simultaneous maximum-likelihood fit to the distribution of the $\text{BDT}_{\text{W}/\text{t}\bar{\text{t}}}$ discriminant in the "2jets 1tag" and "3jets 2tags" categories.

Process	t	$\bar{\text{t}}$	$\text{t} + \bar{\text{t}}$
$\text{t}\bar{\text{t}}$	1543 ± 24	1573 ± 23	3118 ± 34
tW	143 ± 8	168 ± 9	311 ± 12
s-channel	44 ± 4	27 ± 3	72 ± 4
W+jets	1332 ± 60	1022 ± 56	2353 ± 81
Z/γ^*+jets	181 ± 23	189 ± 23	371 ± 32
Diboson	21 ± 2	13 ± 1	33 ± 2
Multijet	219 ± 110	208 ± 105	427 ± 214
t-channel	3852 ± 101	2202 ± 90	6049 ± 136
Total expected	7334 ± 165	5402 ± 153	12733 ± 271
Data	7223	5281	12504

Table 2. The expected number of signal and background events in the "2jets 1tag" signal region ($\text{BDT}_{\text{W}/\text{t}\bar{\text{t}}} > 0.45$) after scaling to the results of the maximum-likelihood fit. The uncertainties reflect the limited number of MC events and the estimated scale factor uncertainties, where appropriate. The multijet events background contribution is estimated using a data-based procedure.

In simulation, the parton-level definition of $\cos\theta_\mu^*$ is defined based on the generated muon from the decay chain of a top quark or antiquark and the spectator quark scattering off the top quark or antiquark via virtual W boson exchange, with all momenta boosted into the rest frame of the generated top quark or antiquark. To preserve the spin information from the W decay, the response matrix takes into account the case in which the muon is from $\text{W} \to \tau\nu \to \mu\nu\nu$ decay by unfolding the angular distribution to the τ lepton. Prior to unfolding, remaining background contributions are subtracted from the reconstructed data, using the fitted number of events and their uncertainties, estimated in section 7.

After the background subtraction, an unfolding procedure [43] is applied. At its core is the application of a matrix inversion using second derivatives for regularisation. A detailed description of the procedure can be found in the $\text{t}\bar{\text{t}}$ charge asymmetry analysis [44], performed previously by CMS, which utilises the same method.

The performance of the unfolding algorithm is checked using sets of pseudo-experiments. Pull distributions show no sign that the uncertainties are treated incorrectly.

A bias test is performed by injecting anomalous Wtb-vertex coupling events as pseudo-data, generated with CompHEP [18, 19]. This test verifies that, with the analysis strategy described here, it is possible to measure different asymmetries correctly, and with only a small bias that will be accounted for as a systematic uncertainty.

The value of A_μ is extracted using a χ^2-fit of the unfolded $\cos\theta_\mu^*$ distribution, under the assumption that eq. (5.1) is valid. The fit takes into account the bin-by-bin correlations that are induced in the unfolding procedure.

An alternative procedure, based on analytic matrix inversion with only two bins in the $\cos\theta_\mu^*$ distribution (corresponding to forward- and backward-going muons), is used as a crosscheck. Although the results of the two methods are in agreement, the expected precision of the analytic matrix inversion is slightly worse when tested using pseudo-data.

9 Systematic uncertainties

The differential cross section and asymmetry measurement presented in this paper can be affected by several sources of systematic uncertainty. To evaluate the impact of each source, we perform a new background estimation and repeat the measurement with systematically shifted simulated templates and response matrices. The expected systematic uncertainty for each source is taken to be the maximal shift in the values of the asymmetry between the nominal asymmetry and the one measured using the shifted templates.

ML fit uncertainty: this uncertainty is determined by propagating the uncertainty associated with the background normalisation from the maximum-likelihood fit through the unfolding procedure.

Other background fractions: a specific uncertainty is assigned to the fraction of each minor process that is combined with similar and larger processes in the fit. These are dibosons and Z/γ^*+jets production for the W/Z/diboson component, and the tW and s-channel production for the top quark component. A yield uncertainty of 50% is used for each of the templates.

Multijet events background shape: a shape uncertainty is taken into account by varying the range of inverted isolation requirement used to extract the templates for estimating this background contribution.

Multijet events background yield: a 50% uncertainty is assigned to the yield obtained from the multijet events fit.

b tagging: the uncertainties in the b tagging and mistagging efficiencies for individual jets as measured in data [35] are propagated to the simulation event weights.

Detector-related jet and $\not{E}_T$ effects: all reconstructed jet four-momenta in simulated events are changed simultaneously according to the η- and p_T-dependent uncertainties in the jet energy scale [38]. The changes in jet four-momenta are also propagated to $\not{E}_T$. In addition, the effect on the measurement of $\not{E}_T$ arising from the 10% uncertainty associated with unclustered energy deposits in the calorimeters is estimated after subtracting from

$\not{E}_T$ all jets and leptons. An extra uncertainty accounts for the known difference in JER relative to data [38].

Pileup: a 5% uncertainty is applied to the average expected number of pileup interactions in order to estimate the uncertainty arising from the modelling of pileup.

Muon trigger, identification, and isolation efficiencies: a systematic uncertainty of 1% is applied independently to the muon trigger, identification, and isolation efficiencies. These uncertainties cover the efficiency differences between the phase space regions sampled by the present selection and by the selection of Z/γ^*+jets events for the tag-and-probe procedure.

$t\bar{t}$ top quark p_T reweighting: the MADGRAPH model for $t\bar{t}$ production is known to predict a harder p_T^t spectrum compared to that observed in data [41, 42]. Although the correlation with other uncertainty sources is not clear, the spectrum of generator-level top quarks in $t\bar{t}$ events is reweighted to the measured differential cross section and an additional systematic uncertainty from this reweighting by either doubling or not using any reweighting is applied.

W boson p_T reweighting in W+jets: the MADGRAPH model for W+jets events predicts a p_T spectrum of the reconstructed W boson candidate that does not agree with data in the "2 jets 0 tags" control region. The distribution is reweighted to data (after subtraction of other processes) and the difference is taken as a systematic uncertainty.

$\cos\theta_\mu^*$ reweighting in W+jets: the uncertainty associated with the reweighting procedure presented in section 6.2 is estimated conservatively by comparing the result after $\cos\theta_\mu^*$ shape reweighting with that determined with no weighting applied. The difference between the two is then symmetrised and taken as the uncertainty. An additional uncertainty is assigned to the fraction of W+jets events in which jets arise from heavy flavours. This uncertainty is taken into account by scaling its contribution by $\pm50\%$ relative to the prediction by MADGRAPH.

Unfolding bias: a test of the analysis shows a small bias when injecting events with anomalous couplings as pseudo-data. This is treated as an additional systematic uncertainty in the asymmetry measurement.

Generator model: the nominal result is compared with the one obtained using an unfolding matrix from a signal sample generated with aMC@NLO, interfaced with PYTHIA 8 for parton showering.

Top quark mass: additional samples of $t\bar{t}$ and signal events are generated with the top quark mass changed by $\pm3\,\text{GeV}$. These are used to determine the uncertainty arising from our knowledge of the top quark mass. This is a conservative estimate as the current world average is $173.3 \pm 0.8\,\text{GeV}$ [45].

Parton distribution functions: the uncertainty due to the choice of the set of parton distribution functions (PDF) is estimated by reweighting the simulated events with each of the 52 eigenvectors of the CT10 collection [46], and additional eigenvectors corresponding to variation of the strong coupling, as well as using the central sets from the MSTW2008CPdeut [47] and NNPDF23 [48] collections. The LHAPDF [49] package is used for the reweighting.

Renormalisation and factorisation scales: the uncertainties in the renormalisation and factorisation scales (set to a common scale equal to the momentum transfer Q in the event) are evaluated for signal, $t\bar{t}$ and W+jets independently, by doubling or halving the value of the scale. For the signal, a reweighting procedure is applied to simulated events, using the simplification of neglecting the scale dependence of the parton shower (PS). Since the signal process does not contain a QCD vertex at LO in the 5FS, the dependence of its cross section with scale Q can be written as

$$\sigma^{\mathrm{LO}}_{t\text{-ch.}}(Q) = \int_0^1 \mathrm{d}x_1 f_{\mathrm{PDF}}(x_1, Q^2) \int_0^1 \mathrm{d}x_2 f_{\mathrm{PDF}}(x_2, Q^2)\, \hat{\sigma}(x_1, x_2), \qquad (9.1)$$

where x_i are the momentum fractions of the two partons in the colliding protons, $f_{\mathrm{PDF}}(x_i, Q^2)$ is the PDF, and $\hat{\sigma}(x_1, x_2)$ denotes the partonic cross section. The event reweighting to a different scale Q' is then defined using a factor

$$w_{Q \to Q'}(x_1, x_2) = \frac{f_{\mathrm{PDF}}(x_1, Q'^2)\, f_{\mathrm{PDF}}(x_2, Q'^2)}{f_{\mathrm{PDF}}(x_1, Q^2)\, f_{\mathrm{PDF}}(x_2, Q^2)}. \qquad (9.2)$$

Dedicated simulated samples with doubled and halved scales are used to verify the validity of the approximation of ignoring the effect of scale in PS simulation for the signal process. The reweighting is preferred over use of these dedicated samples because of their limited number of events.

For the $t\bar{t}$ and W+jets backgrounds, a lower threshold is applied to the $\mathrm{BDT}_{\mathrm{W}/t\bar{t}}$ discriminant in simulated samples that have a changed Q scale to increase the number of selected events. This provides a $\cos\theta^*_\mu$ distribution that agrees, within the limited statistical uncertainty of the simulation, with the shape obtained by applying the nominal $\mathrm{BDT}_{\mathrm{W}/t\bar{t}}$ discriminant threshold.

Matrix element/parton shower matching threshold: the impact of the choice of ME/PS matching threshold in the MLM procedure is evaluated independently for $t\bar{t}$ and W+jets processes, using dedicated samples in which the threshold is either doubled or halved.

Limited number of simulated events: the uncertainty associated with the limited amount of simulated events used in forming the templates is taken into account at all stages of the analysis, i.e. both in terms of fluctuations in the background and in determining the elements of the migration matrix. The limited number of simulated events can also influence the estimation of other systematic uncertainties, potentially leading to an overestimation of the associated uncertainties.

Table 3 shows the impact of the different sources of systematic uncertainties on the asymmetry measurements.

	$\delta A_\mu(\mathrm{t})/10^{-2}$	$\delta A_\mu(\bar{\mathrm{t}})/10^{-2}$	$\delta A_\mu(\mathrm{t}+\bar{\mathrm{t}})/10^{-2}$
Statistical	3.2	4.6	2.6
ML fit uncertainty	0.7	1.2	0.6
Diboson bkg. fraction	<0.1	<0.1	<0.1
Z/γ^*+jets bkg. fraction	<0.1	<0.1	<0.1
s-channel bkg. fraction	0.3	0.2	0.2
tW bkg. fraction	0.1	0.7	0.2
Multijet events shape	0.5	0.7	0.5
Multijet events yield	1.9	1.2	1.7
b tagging	0.7	1.2	0.9
Mistagging	<0.1	0.1	<0.1
Jet energy resolution	2.7	1.8	2.0
Jet energy scale	1.3	2.6	1.1
Unclustered $\not{E}_T$	1.1	3.3	1.3
Pileup	0.3	0.2	0.2
Lepton identification	<0.1	<0.1	<0.1
Lepton isolation	<0.1	<0.1	<0.1
Muon trigger efficiency	<0.1	<0.1	<0.1
Top quark p_T reweighting	0.3	0.3	0.3
W+jets W boson p_T reweighting	0.1	0.1	0.1
W+jets heavy-flavour fraction	4.7	6.2	5.3
W+jets light-flavour fraction	<0.1	<0.1	0.1
W+jets $\cos\theta_\mu^*$ reweighting	2.9	3.4	3.1
Unfolding bias	2.5	4.2	3.1
Generator model	1.6	3.5	0.3
Top quark mass	1.9	2.9	1.8
PDF	0.9	1.6	1.2
t-channel renorm./fact. scales	0.2	0.2	0.2
$t\bar{t}$ renorm./fact. scales	2.2	3.4	2.7
$t\bar{t}$ ME/PS matching	2.2	0.5	1.6
W+jets renorm./fact. scales	3.7	4.6	4.0
W+jets ME/PS matching	3.8	3.0	3.4
Limited MC events	2.1	3.2	1.8
Total uncertainty	10.5	13.8	10.5

Table 3. List of systematic uncertainties and their induced shifts from the nominal measured asymmetry for the top quark ($\delta A_\mu(\mathrm{t})$), antiquark ($\delta A_\mu(\bar{\mathrm{t}})$), and their combination ($\delta A_\mu(\mathrm{t}+\bar{\mathrm{t}})$).
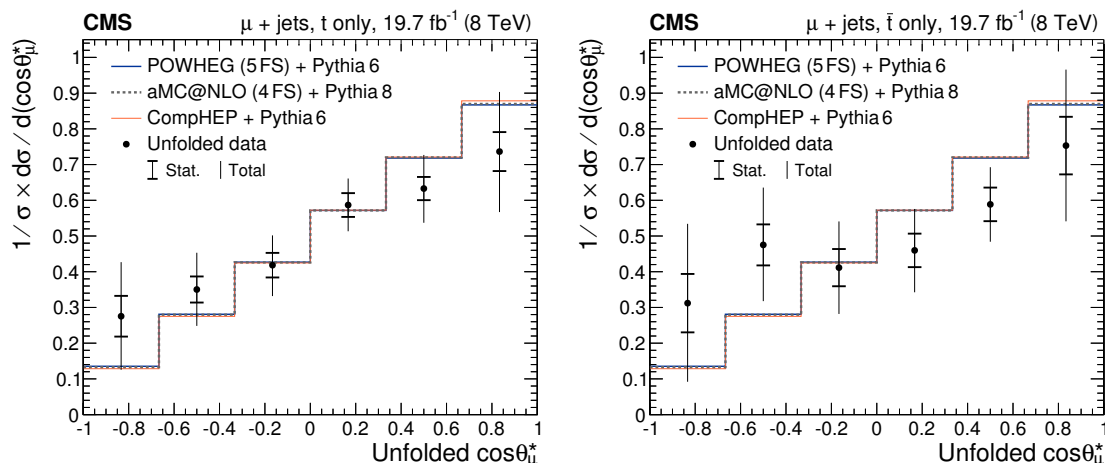
Figure 6. The normalised differential cross sections as a function of unfolded $\cos \theta_\mu^*$ for (left) top quark and (right) antiquark compared to the predictions from POWHEG, aMC@NLO, and CompHEP. The inner (outer) bars represent the statistical (total) uncertainties.

10 Results

Figures 6 and 7, respectively, show the differential cross sections obtained from the unfolding procedure for single top quark and antiquark production, and for their combination, with a comparison to the SM expectations from POWHEG, aMC@NLO, and CompHEP. These generators agree well in their predictions of A_μ. Uncertainties arising from the renormalisation and factorisation scale and PDF variations have been found to be negligible for the predicted differential distributions and are therefore not shown.

The asymmetry A_μ is extracted from the differential cross section according to eq. (5.1), taking into account correlations. Using this procedure, we obtain:

$$A_\mu(\mathrm{t}) = 0.29 \pm 0.03\,(\mathrm{stat}) \pm 0.10\,(\mathrm{syst}) = 0.29 \pm 0.11, \tag{10.1}$$

$$A_\mu(\bar{\mathrm{t}}) = 0.21 \pm 0.05\,(\mathrm{stat}) \pm 0.13\,(\mathrm{syst}) = 0.21 \pm 0.14, \tag{10.2}$$

$$A_\mu(\mathrm{t}+\bar{\mathrm{t}}) = 0.26 \pm 0.03\,(\mathrm{stat}) \pm 0.10\,(\mathrm{syst}) = 0.26 \pm 0.11, \tag{10.3}$$

where the combined result is compatible with a p-value of $p(\mathrm{data}|\mathrm{SM}) = 4.6\%$, which corresponds to 2.0 standard deviations compared to the expected SM asymmetry of 0.44 as predicted by POWHEG (NLO). Alternatively, the compatibility of the combined result with the hypothetical case of $A_\mu = 0$ is smaller, yielding a p-value of $p(\mathrm{data}|A_\mu = 0) = 0.7\%$, and corresponding to 2.7 standard deviations. The SM asymmetry predictions for simulated top quark and antiquark events are equal, while [1] predicts a $\mathcal{O}(1\%)$ difference, which is small compared to the precision of the current measurement.

As a crosscheck, an analytic 2-bin unfolding is also performed, which yields the numbers $N(\uparrow)$ and $N(\downarrow)$ defined in eq. (1.1). This gives a compatible but slightly less precise value for A_μ of:

$$A_\mu(\mathrm{t}+\bar{\mathrm{t}}) = 0.28 \pm 0.03\,(\mathrm{stat}) \pm 0.1\,(\mathrm{syst}) = 0.28 \pm 0.12. \tag{10.4}$$
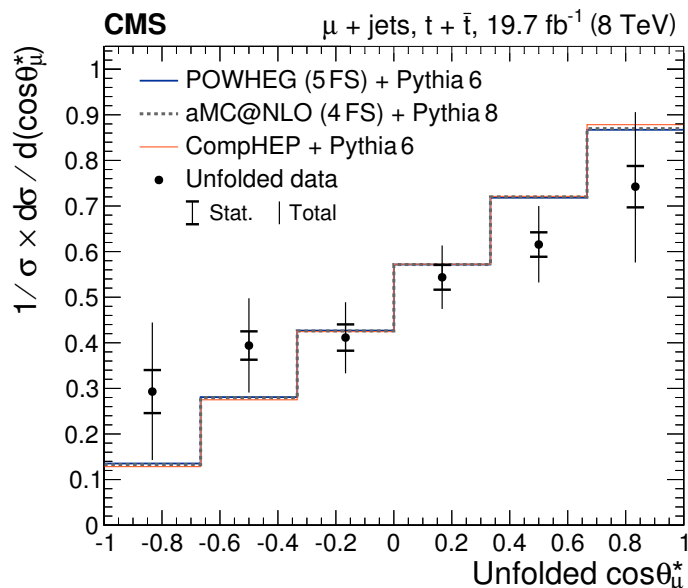
Figure 7. The normalised differential cross section as a function of unfolded $\cos\theta_\mu^*$ for top quark and antiquark combined, compared to the predictions from POWHEG, aMC@NLO, and COMPHEP. The inner (outer) bars represent the statistical (total) uncertainties.

11 Summary

The first measurement of the top quark spin asymmetry, sensitive to the top quark polarisation, in t-channel single top quark production has been presented. This measurement is based on a sample of pp collisions at a centre-of-mass energy of 8 TeV, corresponding to an integrated luminosity of 19.7 fb^{-1}.

The asymmetry, A_μ, is obtained by performing a differential cross section measurement of $\cos\theta_\mu^*$, between forward- and backward-going muons with respect to the direction of the spectator quark in the top quark rest frame. The measurement yields $A_\mu = 0.26 \pm 0.03\,(\text{stat}) \pm 0.10\,(\text{syst}) = 0.26 \pm 0.11$, which is compatible with a p-value of 4.6%, equivalent to 2.0 standard deviations, with the standard model expectation.

The asymmetry observed in data is smaller than the prediction. Separate results from exclusive top quark or antiquark events are compatible within the uncertainties. This difference cannot be explained by any single source of systematic uncertainty considered in this analysis.

Acknowledgments

References

[1] G. Mahlon and S.J. Parke, *Single top quark production at the LHC: understanding spin*, *Phys. Lett.* **B 476** (2000) 323 [hep-ph/9912458] [INSPIRE].

[2] M. Jezabek and J.H. Kuhn, *V-A tests through leptons from polarized top quarks*, *Phys. Lett.* **B 329** (1994) 317 [hep-ph/9403366] [INSPIRE].

[3] J.A. Aguilar-Saavedra and J. Bernabeu, *W polarisation beyond helicity fractions in top quark decays*, *Nucl. Phys.* **B 840** (2010) 349 [arXiv:1005.5382] [INSPIRE].

[4] J.A. Aguilar-Saavedra, *Single top quark production at LHC with anomalous Wtb couplings*, *Nucl. Phys.* **B 804** (2008) 160 [arXiv:0803.3810] [INSPIRE].

[5] J.A. Aguilar-Saavedra, *A minimal set of top anomalous couplings*, *Nucl. Phys.* **B 812** (2009) 181 [arXiv:0811.3842] [INSPIRE].

[6] F. Bach and T. Ohl, *Anomalous top couplings at hadron colliders revisited*, *Phys. Rev.* **D 86** (2012) 114026 [arXiv:1209.4564] [INSPIRE].

[7] CMS collaboration, *The CMS experiment at the CERN LHC*, 2008 *JINST* **3** S08004 [INSPIRE].

[8] CMS collaboration, *Particle-flow event reconstruction in CMS and performance for jets, taus and MET*, CMS-PAS-PFT-09-001 (2009).

[9] CMS collaboration, *Commissioning of the particle-flow event reconstruction with the first LHC collisions recorded in the CMS detector*, CMS-PAS-PFT-10-001 (2010).

[10] CMS collaboration, *CMS luminosity based on pixel cluster counting — Summer 2013 update*, CMS-PAS-LUM-13-001 (2013).

[11] S. Alioli, P. Nason, C. Oleari and E. Re, *A general framework for implementing NLO calculations in shower Monte Carlo programs: the POWHEG BOX*, *JHEP* **06** (2010) 043 [arXiv:1002.2581] [INSPIRE].

[12] S. Alioli, P. Nason, C. Oleari and E. Re, *NLO single-top production matched with shower in POWHEG: s- and t-channel contributions*, *JHEP* **09** (2009) 111 [*Erratum ibid.* **1002** (2010) 011] [arXiv:0907.4076] [INSPIRE].

[13] S. Frixione, P. Nason and C. Oleari, *Matching NLO QCD computations with Parton Shower simulations: the POWHEG method*, *JHEP* **11** (2007) 070 [arXiv:0709.2092] [INSPIRE].

[14] T. Sjöstrand, S. Mrenna and P.Z. Skands, *PYTHIA 6.4 physics and manual*, *JHEP* **05** (2006) 026 [hep-ph/0603175] [INSPIRE].

[15] S. Jadach, J.H. Kuhn and Z. Wąs, *TAUOLA: a library of Monte Carlo programs to simulate decays of polarized τ leptons*, *Comput. Phys. Commun.* **64** (1990) 275 [INSPIRE].

[16] J. Alwall et al., *The automated computation of tree-level and next-to-leading order differential cross sections and their matching to parton shower simulations*, *JHEP* **07** (2014) 079 [arXiv:1405.0301] [INSPIRE].

[17] T. Sjöstrand et al., *An introduction to PYTHIA 8.2*, *Comput. Phys. Commun.* **191** (2015) 159 [arXiv:1410.3012] [INSPIRE].

[18] COMPHEP collaboration, E. Boos et al., *CompHEP 4.4: automatic computations from Lagrangians to events*, *Nucl. Instrum. Meth.* **A 534** (2004) 250 [hep-ph/0403113] [INSPIRE].

[19] E.E. Boos, V.E. Bunichev, L.V. Dudko, V.I. Savrin and A.V. Sherstnev, *Method for simulating electroweak top-quark production events in the NLO approximation: singleTop event generator*, *Phys. Atom. Nucl.* **69** (2006) 1317 [INSPIRE].

[20] F. Maltoni and T. Stelzer, *MadEvent: automatic event generation with MadGraph*, *JHEP* **02** (2003) 027 [hep-ph/0208156] [INSPIRE].

[21] M.L. Mangano, M. Moretti, F. Piccinini and M. Treccani, *Matching matrix elements and shower evolution for top-quark production in hadronic collisions*, *JHEP* **01** (2007) 013 [hep-ph/0611129] [INSPIRE].

[22] J. Alwall et al., *Comparative study of various algorithms for the merging of parton showers and matrix elements in hadronic collisions*, *Eur. Phys. J.* **C 53** (2008) 473 [arXiv:0706.2569] [INSPIRE].

[23] S. Hoche, F. Krauss, M. Schonherr and F. Siegert, *Automating the POWHEG method in Sherpa*, *JHEP* **04** (2011) 024 [arXiv:1008.5399] [INSPIRE].

[24] S. Höche, F. Krauss, M. Schönherr and F. Siegert, *W + n-Jet predictions at the Large Hadron Collider at next-to-leading order matched with a parton shower*, *Phys. Rev. Lett.* **110** (2013) 052001 [arXiv:1201.5882] [INSPIRE].

[25] N. Kidonakis, *Differential and total cross sections for top pair and single top production*, in the proceedings of the 20th *International Workshop on Deep-Inelastic Scattering and Related Subjects (DIS 2012)*, June 11-15, New Castle, U.K. (2012), arXiv:1205.3453 [INSPIRE].

[26] M. Czakon and A. Mitov, *Top++: a program for the calculation of the top-pair cross-section at hadron colliders*, *Comput. Phys. Commun.* **185** (2014) 2930 [arXiv:1112.5675] [INSPIRE].

[27] R. Gavin, Y. Li, F. Petriello and S. Quackenbush, *FEWZ 2.0: a code for hadronic Z production at next-to-next-to-leading order*, *Comput. Phys. Commun.* **182** (2011) 2388 [arXiv:1011.3540] [INSPIRE].

[28] J.M. Campbell and R.K. Ellis, *MCFM for the Tevatron and the LHC*, *Nucl. Phys. Proc. Suppl.* **205-206** (2010) 10 [arXiv:1007.3492] [INSPIRE].

[29] GEANT4 collaboration, S. Agostinelli et al., *GEANT4 – A simulation toolkit*, *Nucl. Instrum. Meth.* **A 506** (2003) 250 [INSPIRE].

[30] CMS collaboration, *Measurement of the single-top-quark t-channel cross section in pp collisions at $\sqrt{s} = 7$ TeV*, *JHEP* **12** (2012) 035 [arXiv:1209.4533] [INSPIRE].

[31] M. Cacciari, G.P. Salam and G. Soyez, *The anti-k_t jet clustering algorithm*, *JHEP* **04** (2008) 063 [arXiv:0802.1189] [INSPIRE].

[32] M. Cacciari, G.P. Salam and G. Soyez, *FastJet user manual*, *Eur. Phys. J.* **C 72** (2012) 1896 [arXiv:1111.6097] [INSPIRE].

[33] CMS collaboration, *Pileup removal algorithms*, CMS-PAS-JME-14-001 (2014).

[34] CMS collaboration, *Identification of b-quark jets with the CMS experiment*, 2013 *JINST* **8** P04013 [arXiv:1211.4462] [INSPIRE].

[35] CMS collaboration, *Performance of b tagging at $\sqrt{s} = 8$ TeV in multijet, ttbar and boosted topology events*, CMS-PAS-BTV-13-001 (2013).

[36] CMS collaboration, *Performance of CMS muon reconstruction in pp collision events at $\sqrt{s} = 7$ TeV*, 2012 *JINST* **7** P10002 [arXiv:1206.4071] [INSPIRE].

[37] CMS collaboration, *Single muon efficiencies in 2012 data*, CMS-DP-2013-009 (2013).

[38] CMS collaboration, *Determination of jet energy calibration and transverse momentum resolution in CMS*, 2011 *JINST* **6** P11002 [arXiv:1107.4277] [INSPIRE].

[39] CMS collaboration, *Measurement of the t-channel single top quark production cross section in pp collisions at $\sqrt{s} = 7$ TeV*, *Phys. Rev. Lett.* **107** (2011) 091802 [arXiv:1106.3052] [INSPIRE].

[40] T. Gleisberg et al., *Event generation with SHERPA 1.1*, *JHEP* **02** (2009) 007 [arXiv:0811.4622] [INSPIRE].

[41] CMS collaboration, *Measurement of differential top-quark pair production cross sections in pp colisions at $\sqrt{s} = 7$ TeV*, *Eur. Phys. J.* **C 73** (2013) 2339 [arXiv:1211.2220] [INSPIRE].

[42] CMS collaboration, *Measurement of the differential cross section for top quark pair production in pp collisions at $\sqrt{s} = 8$ TeV*, *Eur. Phys. J.* **C 75** (2015) 542 [arXiv:1505.04480] [INSPIRE].

[43] V. Blobel, *An unfolding method for high-energy physics experiments*, hep-ex/0208022 [INSPIRE].

[44] CMS collaboration, *Measurement of the charge asymmetry in top-quark pair production in proton-proton collisions at $\sqrt{s} = 7$ TeV*, *Phys. Lett.* **B 709** (2012) 28 [arXiv:1112.5100] [INSPIRE].

[45] ATLAS, CDF, CMS, D0 collaboration, *First combination of Tevatron and LHC measurements of the top-quark mass*, arXiv:1403.4427 [INSPIRE].

[46] H.-L. Lai et al., *New parton distributions for collider physics*, *Phys. Rev.* **D 82** (2010) 074024 [arXiv:1007.2241] [INSPIRE].

[47] A.D. Martin, A.J. T.M. Mathijssen, W.J. Stirling, R.S. Thorne, B.J.A. Watt and G. Watt, *Extended parameterisations for MSTW PDFs and their effect on Lepton Charge Asymmetry from W decays*, *Eur. Phys. J.* **C 73** (2013) 2318 [arXiv:1211.1215] [INSPIRE].

[48] R.D. Ball et al., *Parton distributions with LHC data*, *Nucl. Phys.* **B 867** (2013) 244 [arXiv:1207.1303] [INSPIRE].

[49] M.R. Whalley, D. Bourilkov and R.C. Group, *The Les Houches accord PDFs (LHAPDF) and LHAGLUE*, hep-ph/0508110 [INSPIRE].

The CMS collaboration

Yerevan Physics Institute, Yerevan, Armenia

V. Khachatryan, A.M. Sirunyan, A. Tumasyan

Institut für Hochenergiephysik der OeAW, Wien, Austria

W. Adam, E. Asilar, T. Bergauer, J. Brandstetter, E. Brondolin, M. Dragicevic, J. Erö, M. Flechl, M. Friedl, R. Frühwirth[1], V.M. Ghete, C. Hartl, N. Hörmann, J. Hrubec, M. Jeitler[1], V. Knünz, A. König, M. Krammer[1], I. Krätschmer, D. Liko, T. Matsushita, I. Mikulec, D. Rabady[2], B. Rahbaran, H. Rohringer, J. Schieck[1], R. Schöfbeck, J. Strauss, W. Treberer-Treberspurg, W. Waltenberger, C.-E. Wulz[1]

National Centre for Particle and High Energy Physics, Minsk, Belarus

V. Mossolov, N. Shumeiko, J. Suarez Gonzalez

Universiteit Antwerpen, Antwerpen, Belgium

S. Alderweireldt, T. Cornelis, E.A. De Wolf, X. Janssen, A. Knutsson, J. Lauwers, S. Luyckx, M. Van De Klundert, H. Van Haevermaet, P. Van Mechelen, N. Van Remortel, A. Van Spilbeeck

Vrije Universiteit Brussel, Brussel, Belgium

S. Abu Zeid, F. Blekman, J. D'Hondt, N. Daci, I. De Bruyn, K. Deroover, N. Heracleous, J. Keaveney, S. Lowette, L. Moreels, A. Olbrechts, Q. Python, D. Strom, S. Tavernier, W. Van Doninck, P. Van Mulders, G.P. Van Onsem, I. Van Parijs

Université Libre de Bruxelles, Bruxelles, Belgium

P. Barria, H. Brun, C. Caillol, B. Clerbaux, G. De Lentdecker, G. Fasanella, L. Favart, A. Grebenyuk, G. Karapostoli, T. Lenzi, A. Léonard, T. Maerschalk, A. Marinov, L. Perniè, A. Randle-conde, T. Seva, C. Vander Velde, P. Vanlaer, R. Yonamine, F. Zenoni, F. Zhang[3]

Ghent University, Ghent, Belgium

K. Beernaert, L. Benucci, A. Cimmino, S. Crucy, D. Dobur, A. Fagot, G. Garcia, M. Gul, J. Mccartin, A.A. Ocampo Rios, D. Poyraz, D. Ryckbosch, S. Salva, M. Sigamani, M. Tytgat, W. Van Driessche, E. Yazgan, N. Zaganidis

Université Catholique de Louvain, Louvain-la-Neuve, Belgium

S. Basegmez, C. Beluffi[4], O. Bondu, S. Brochet, G. Bruno, A. Caudron, L. Ceard, G.G. Da Silveira, C. Delaere, D. Favart, L. Forthomme, A. Giammanco[5], J. Hollar, A. Jafari, P. Jez, M. Komm, V. Lemaitre, A. Mertens, M. Musich, C. Nuttens, L. Perrini, A. Pin, K. Piotrzkowski, A. Popov[6], L. Quertenmont, M. Selvaggi, M. Vidal Marono

Université de Mons, Mons, Belgium

N. Beliy, G.H. Hammad

Centro Brasileiro de Pesquisas Fisicas, Rio de Janeiro, Brazil

W.L. Aldá Júnior, F.L. Alves, G.A. Alves, L. Brito, M. Correa Martins Junior, M. Hamer, C. Hensel, C. Mora Herrera, A. Moraes, M.E. Pol, P. Rebello Teles

Universidade do Estado do Rio de Janeiro, Rio de Janeiro, Brazil

E. Belchior Batista Das Chagas, W. Carvalho, J. Chinellato[7], A. Custódio, E.M. Da Costa, D. De Jesus Damiao, C. De Oliveira Martins, S. Fonseca De Souza, L.M. Huertas Guativa, H. Malbouisson, D. Matos Figueiredo, L. Mundim, H. Nogima, W.L. Prado Da Silva, A. Santoro, A. Sznajder, E.J. Tonelli Manganote[7], A. Vilela Pereira

Universidade Estadual Paulista [a], Universidade Federal do ABC [b], São Paulo, Brazil

S. Ahuja[a], C.A. Bernardes[b], A. De Souza Santos[b], S. Dogra[a], T.R. Fernandez Perez Tomei[a], E.M. Gregores[b], P.G. Mercadante[b], C.S. Moon[a,8], S.F. Novaes[a], Sandra S. Padula[a], D. Romero Abad, J.C. Ruiz Vargas

Institute for Nuclear Research and Nuclear Energy, Sofia, Bulgaria

A. Aleksandrov, R. Hadjiiska, P. Iaydjiev, M. Rodozov, S. Stoykova, G. Sultanov, M. Vutova

University of Sofia, Sofia, Bulgaria

A. Dimitrov, I. Glushkov, L. Litov, B. Pavlov, P. Petkov

Institute of High Energy Physics, Beijing, China

M. Ahmad, J.G. Bian, G.M. Chen, H.S. Chen, M. Chen, T. Cheng, R. Du, C.H. Jiang, R. Plestina[9], F. Romeo, S.M. Shaheen, A. Spiezia, J. Tao, C. Wang, Z. Wang, H. Zhang

State Key Laboratory of Nuclear Physics and Technology, Peking University, Beijing, China

C. Asawatangtrakuldee, Y. Ban, Q. Li, S. Liu, Y. Mao, S.J. Qian, D. Wang, Z. Xu

Universidad de Los Andes, Bogota, Colombia

C. Avila, A. Cabrera, L.F. Chaparro Sierra, C. Florez, J.P. Gomez, B. Gomez Moreno, J.C. Sanabria

University of Split, Faculty of Electrical Engineering, Mechanical Engineering and Naval Architecture, Split, Croatia

N. Godinovic, D. Lelas, I. Puljak, P.M. Ribeiro Cipriano

University of Split, Faculty of Science, Split, Croatia

Z. Antunovic, M. Kovac

Institute Rudjer Boskovic, Zagreb, Croatia

V. Brigljevic, K. Kadija, J. Luetic, S. Micanovic, L. Sudic

University of Cyprus, Nicosia, Cyprus

A. Attikis, G. Mavromanolakis, J. Mousa, C. Nicolaou, F. Ptochos, P.A. Razis, H. Rykaczewski

Charles University, Prague, Czech Republic

M. Bodlak, M. Finger[10], M. Finger Jr.[10]

Academy of Scientific Research and Technology of the Arab Republic of Egypt, Egyptian Network of High Energy Physics, Cairo, Egypt

A.A. Abdelalim[11,12], A. Awad, M. El Sawy[13,14], A. Mahrous[11], A. Radi[14,15]

National Institute of Chemical Physics and Biophysics, Tallinn, Estonia

B. Calpas, M. Kadastik, M. Murumaa, M. Raidal, A. Tiko, C. Veelken

Department of Physics, University of Helsinki, Helsinki, Finland

P. Eerola, J. Pekkanen, M. Voutilainen

Helsinki Institute of Physics, Helsinki, Finland

J. Härkönen, V. Karimäki, R. Kinnunen, T. Lampén, K. Lassila-Perini, S. Lehti, T. Lindén, P. Luukka, T. Mäenpää, T. Peltola, E. Tuominen, J. Tuominiemi, E. Tuovinen, L. Wendland

Lappeenranta University of Technology, Lappeenranta, Finland

J. Talvitie, T. Tuuva

DSM/IRFU, CEA/Saclay, Gif-sur-Yvette, France

M. Besancon, F. Couderc, M. Dejardin, D. Denegri, B. Fabbro, J.L. Faure, C. Favaro, F. Ferri, S. Ganjour, A. Givernaud, P. Gras, G. Hamel de Monchenault, P. Jarry, E. Locci, M. Machet, J. Malcles, J. Rander, A. Rosowsky, M. Titov, A. Zghiche

Laboratoire Leprince-Ringuet, Ecole Polytechnique, IN2P3-CNRS, Palaiseau, France

I. Antropov, S. Baffioni, F. Beaudette, P. Busson, L. Cadamuro, E. Chapon, C. Charlot, T. Dahms, O. Davignon, N. Filipovic, A. Florent, R. Granier de Cassagnac, M. Jo, S. Lisniak, L. Mastrolorenzo, P. Miné, I.N. Naranjo, M. Nguyen, C. Ochando, G. Ortona, P. Paganini, P. Pigard, S. Regnard, R. Salerno, J.B. Sauvan, Y. Sirois, T. Strebler, Y. Yilmaz, A. Zabi

Institut Pluridisciplinaire Hubert Curien, Université de Strasbourg, Université de Haute Alsace Mulhouse, CNRS/IN2P3, Strasbourg, France

J.-L. Agram[16], J. Andrea, A. Aubin, D. Bloch, J.-M. Brom, M. Buttignol, E.C. Chabert, N. Chanon, C. Collard, E. Conte[16], X. Coubez, J.-C. Fontaine[16], D. Gelé, U. Goerlach, C. Goetzmann, A.-C. Le Bihan, J.A. Merlin[2], K. Skovpen, P. Van Hove

Centre de Calcul de l'Institut National de Physique Nucleaire et de Physique des Particules, CNRS/IN2P3, Villeurbanne, France

S. Gadrat

Université de Lyon, Université Claude Bernard Lyon 1, CNRS-IN2P3, Institut de Physique Nucléaire de Lyon, Villeurbanne, France

S. Beauceron, C. Bernet, G. Boudoul, E. Bouvier, C.A. Carrillo Montoya, R. Chierici, D. Contardo, B. Courbon, P. Depasse, H. El Mamouni, J. Fan, J. Fay, S. Gascon, M. Gouzevitch, B. Ille, F. Lagarde, I.B. Laktineh, M. Lethuillier, L. Mirabito, A.L. Pequegnot, S. Perries, J.D. Ruiz Alvarez, D. Sabes, L. Sgandurra, V. Sordini, M. Vander Donckt, P. Verdier, S. Viret

Georgian Technical University, Tbilisi, Georgia

T. Toriashvili[17]

Tbilisi State University, Tbilisi, Georgia

Z. Tsamalaidze[10]

RWTH Aachen University, I. Physikalisches Institut, Aachen, Germany

C. Autermann, S. Beranek, M. Edelhoff, L. Feld, A. Heister, M.K. Kiesel, K. Klein, M. Lipinski, A. Ostapchuk, M. Preuten, F. Raupach, S. Schael, J.F. Schulte, T. Verlage, H. Weber, B. Wittmer, V. Zhukov[6]

RWTH Aachen University, III. Physikalisches Institut A, Aachen, Germany

M. Ata, M. Brodski, E. Dietz-Laursonn, D. Duchardt, M. Endres, M. Erdmann, S. Erdweg, T. Esch, R. Fischer, A. Güth, T. Hebbeker, C. Heidemann, K. Hoepfner, S. Knutzen, P. Kreuzer, M. Merschmeyer, A. Meyer, P. Millet, M. Olschewski, K. Padeken, P. Papacz, T. Pook, M. Radziej, H. Reithler, M. Rieger, F. Scheuch, L. Sonnenschein, D. Teyssier, S. Thüer

RWTH Aachen University, III. Physikalisches Institut B, Aachen, Germany

V. Cherepanov, Y. Erdogan, G. Flügge, H. Geenen, M. Geisler, F. Hoehle, B. Kargoll, T. Kress, Y. Kuessel, A. Künsken, J. Lingemann, A. Nehrkorn, A. Nowack, I.M. Nugent, C. Pistone, O. Pooth, A. Stahl

Deutsches Elektronen-Synchrotron, Hamburg, Germany

M. Aldaya Martin, I. Asin, N. Bartosik, O. Behnke, U. Behrens, A.J. Bell, K. Borras[18], A. Burgmeier, A. Campbell, S. Choudhury[19], F. Costanza, C. Diez Pardos, G. Dolinska, S. Dooling, T. Dorland, G. Eckerlin, D. Eckstein, T. Eichhorn, G. Flucke, E. Gallo[20], J. Garay Garcia, A. Geiser, A. Gizhko, P. Gunnellini, J. Hauk, M. Hempel[21], H. Jung, A. Kalogeropoulos, O. Karacheban[21], M. Kasemann, P. Katsas, J. Kieseler, C. Kleinwort, I. Korol, W. Lange, J. Leonard, K. Lipka, A. Lobanov, W. Lohmann[21], R. Mankel, I. Marfin[21], I.-A. Melzer-Pellmann, A.B. Meyer, G. Mittag, J. Mnich, A. Mussgiller, S. Naumann-Emme, A. Nayak, E. Ntomari, H. Perrey, D. Pitzl, R. Placakyte, A. Raspereza, B. Roland, M.Ö. Sahin, P. Saxena, T. Schoerner-Sadenius, M. Schröder, C. Seitz, S. Spannagel, K.D. Trippkewitz, R. Walsh, C. Wissing

University of Hamburg, Hamburg, Germany

V. Blobel, M. Centis Vignali, A.R. Draeger, J. Erfle, E. Garutti, K. Goebel, D. Gonzalez, M. Görner, J. Haller, M. Hoffmann, R.S. Höing, A. Junkes, R. Klanner, R. Kogler, N. Kovalchuk, T. Lapsien, T. Lenz, I. Marchesini, D. Marconi, M. Meyer, D. Nowatschin, J. Ott, F. Pantaleo[2], T. Peiffer, A. Perieanu, N. Pietsch, J. Poehlsen, D. Rathjens, C. Sander, C. Scharf, H. Schettler, P. Schleper, E. Schlieckau, A. Schmidt, J. Schwandt, V. Sola, H. Stadie, G. Steinbrück, H. Tholen, D. Troendle, E. Usai, L. Vanelderen, A. Vanhoefer, B. Vormwald

Institut für Experimentelle Kernphysik, Karlsruhe, Germany

M. Akbiyik, C. Barth, C. Baus, J. Berger, C. Böser, E. Butz, T. Chwalek, F. Colombo, W. De Boer, A. Descroix, A. Dierlamm, S. Fink, F. Frensch, R. Friese, M. Gif-

fels, A. Gilbert, D. Haitz, F. Hartmann[2], S.M. Heindl, U. Husemann, I. Katkov[6], A. Kornmayer[2], P. Lobelle Pardo, B. Maier, H. Mildner, M.U. Mozer, T. Müller, Th. Müller, M. Plagge, G. Quast, K. Rabbertz, S. Röcker, F. Roscher, G. Sieber, H.J. Simonis, F.M. Stober, R. Ulrich, J. Wagner-Kuhr, S. Wayand, M. Weber, T. Weiler, C. Wöhrmann, R. Wolf

Institute of Nuclear and Particle Physics (INPP), NCSR Demokritos, Aghia Paraskevi, Greece

G. Anagnostou, G. Daskalakis, T. Geralis, V.A. Giakoumopoulou, A. Kyriakis, D. Loukas, A. Psallidas, I. Topsis-Giotis

University of Athens, Athens, Greece

A. Agapitos, S. Kesisoglou, A. Panagiotou, N. Saoulidou, E. Tziaferi

University of Ioánnina, Ioánnina, Greece

I. Evangelou, G. Flouris, C. Foudas, P. Kokkas, N. Loukas, N. Manthos, I. Papadopoulos, E. Paradas, J. Strologas

Wigner Research Centre for Physics, Budapest, Hungary

G. Bencze, C. Hajdu, A. Hazi, P. Hidas, D. Horvath[22], F. Sikler, V. Veszpremi, G. Vesztergombi[23], A.J. Zsigmond

Institute of Nuclear Research ATOMKI, Debrecen, Hungary

N. Beni, S. Czellar, J. Karancsi[24], J. Molnar, Z. Szillasi[2]

University of Debrecen, Debrecen, Hungary

M. Bartók[25], A. Makovec, P. Raics, Z.L. Trocsanyi, B. Ujvari

National Institute of Science Education and Research, Bhubaneswar, India

P. Mal, K. Mandal, D.K. Sahoo, N. Sahoo, S.K. Swain

Panjab University, Chandigarh, India

S. Bansal, S.B. Beri, V. Bhatnagar, R. Chawla, R. Gupta, U.Bhawandeep, A.K. Kalsi, A. Kaur, M. Kaur, R. Kumar, A. Mehta, M. Mittal, J.B. Singh, G. Walia

University of Delhi, Delhi, India

Ashok Kumar, A. Bhardwaj, B.C. Choudhary, R.B. Garg, A. Kumar, S. Malhotra, M. Naimuddin, N. Nishu, K. Ranjan, R. Sharma, V. Sharma

Saha Institute of Nuclear Physics, Kolkata, India

S. Bhattacharya, K. Chatterjee, S. Dey, S. Dutta, Sa. Jain, N. Majumdar, A. Modak, K. Mondal, S. Mukherjee, S. Mukhopadhyay, A. Roy, D. Roy, S. Roy Chowdhury, S. Sarkar, M. Sharan

Bhabha Atomic Research Centre, Mumbai, India

A. Abdulsalam, R. Chudasama, D. Dutta, V. Jha, V. Kumar, A.K. Mohanty[2], L.M. Pant, P. Shukla, A. Topkar

Tata Institute of Fundamental Research, Mumbai, India

T. Aziz, S. Banerjee, S. Bhowmik[26], R.M. Chatterjee, R.K. Dewanjee, S. Dugad, S. Ganguly, S. Ghosh, M. Guchait, A. Gurtu[27], G. Kole, S. Kumar, B. Mahakud, M. Maity[26], G. Majumder, K. Mazumdar, S. Mitra, G.B. Mohanty, B. Parida, T. Sarkar[26], N. Sur, B. Sutar, N. Wickramage[28]

Indian Institute of Science Education and Research (IISER), Pune, India

S. Chauhan, S. Dube, K. Kothekar, S. Sharma

Institute for Research in Fundamental Sciences (IPM), Tehran, Iran

H. Bakhshiansohi, H. Behnamian, S.M. Etesami[29], A. Fahim[30], R. Goldouzian, M. Khakzad, M. Mohammadi Najafabadi, M. Naseri, S. Paktinat Mehdiabadi, F. Rezaei Hosseinabadi, B. Safarzadeh[31], M. Zeinali

University College Dublin, Dublin, Ireland

M. Felcini, M. Grunewald

INFN Sezione di Bari [a], Università di Bari [b], Politecnico di Bari [c], Bari, Italy

M. Abbrescia[a,b], C. Calabria[a,b], C. Caputo[a,b], A. Colaleo[a], D. Creanza[a,c], L. Cristella[a,b], N. De Filippis[a,c], M. De Palma[a,b], L. Fiore[a], G. Iaselli[a,c], G. Maggi[a,c], M. Maggi[a], G. Miniello[a,b], S. My[a,c], S. Nuzzo[a,b], A. Pompili[a,b], G. Pugliese[a,c], R. Radogna[a,b], A. Ranieri[a], G. Selvaggi[a,b], L. Silvestris[a,2], R. Venditti[a,b], P. Verwilligen[a]

INFN Sezione di Bologna [a], Università di Bologna [b], Bologna, Italy

G. Abbiendi[a], C. Battilana[2], A.C. Benvenuti[a], D. Bonacorsi[a,b], S. Braibant-Giacomelli[a,b], L. Brigliadori[a,b], R. Campanini[a,b], P. Capiluppi[a,b], A. Castro[a,b], F.R. Cavallo[a], S.S. Chhibra[a,b], G. Codispoti[a,b], M. Cuffiani[a,b], G.M. Dallavalle[a], F. Fabbri[a], A. Fanfani[a,b], D. Fasanella[a,b], P. Giacomelli[a], C. Grandi[a], L. Guiducci[a,b], S. Marcellini[a], G. Masetti[a], A. Montanari[a], F.L. Navarria[a,b], A. Perrotta[a], A.M. Rossi[a,b], T. Rovelli[a,b], G.P. Siroli[a,b], N. Tosi[a,b,2], R. Travaglini[a,b]

INFN Sezione di Catania [a], Università di Catania [b], Catania, Italy

G. Cappello[a], M. Chiorboli[a,b], S. Costa[a,b], A. Di Mattia[a], F. Giordano[a,b], R. Potenza[a,b], A. Tricomi[a,b], C. Tuve[a,b]

INFN Sezione di Firenze [a], Università di Firenze [b], Firenze, Italy

G. Barbagli[a], V. Ciulli[a,b], C. Civinini[a], R. D'Alessandro[a,b], E. Focardi[a,b], S. Gonzi[a,b], V. Gori[a,b], P. Lenzi[a,b], M. Meschini[a], S. Paoletti[a], G. Sguazzoni[a], A. Tropiano[a,b], L. Viliani[a,b,2]

INFN Laboratori Nazionali di Frascati, Frascati, Italy

L. Benussi, S. Bianco, F. Fabbri, D. Piccolo, F. Primavera[2]

INFN Sezione di Genova [a], Università di Genova [b], Genova, Italy

V. Calvelli[a,b], F. Ferro[a], M. Lo Vetere[a,b], M.R. Monge[a,b], E. Robutti[a], S. Tosi[a,b]

INFN Sezione di Milano-Bicocca ^{a}, Università di Milano-Bicocca ^{b}, Milano, Italy

L. Brianza, M.E. Dinardo^{a,b}, S. Fiorendi^{a,b}, S. Gennai^a, R. Gerosa^{a,b}, A. Ghezzi^{a,b}, P. Govoni^{a,b}, S. Malvezzi^a, R.A. Manzoni^{a,b,2}, B. Marzocchi^{a,b,2}, D. Menasce^a, L. Moroni^a, M. Paganoni^{a,b}, D. Pedrini^a, S. Ragazzi^{a,b}, N. Redaelli^a, T. Tabarelli de Fatis^{a,b}

INFN Sezione di Napoli ^{a}, Università di Napoli 'Federico II' ^{b}, Napoli, Italy, Università della Basilicata ^{c}, Potenza, Italy, Università G. Marconi ^{d}, Roma, Italy

S. Buontempo^a, N. Cavallo^{a,c}, S. Di Guida^{a,d,2}, M. Esposito^{a,b}, F. Fabozzi^{a,c}, A.O.M. Iorio^{a,b}, G. Lanza^a, L. Lista^a, S. Meola^{a,d,2}, M. Merola^a, P. Paolucci^{a,2}, C. Sciacca^{a,b}, F. Thyssen

INFN Sezione di Padova ^{a}, Università di Padova ^{b}, Padova, Italy, Università di Trento ^{c}, Trento, Italy

P. Azzi^{a,2}, N. Bacchetta^a, L. Benato^{a,b}, D. Bisello^{a,b}, A. Boletti^{a,b}, R. Carlin^{a,b}, P. Checchia^a, M. Dall'Osso^{a,b,2}, T. Dorigo^a, U. Dosselli^a, F. Fanzago^a, F. Gasparini^{a,b}, U. Gasparini^{a,b}, F. Gonella^a, A. Gozzelino^a, S. Lacaprara^a, M. Margoni^{a,b}, A.T. Meneguzzo^{a,b}, F. Montecassiano^a, J. Pazzini^{a,b,2}, N. Pozzobon^{a,b}, P. Ronchese^{a,b}, F. Simonetto^{a,b}, E. Torassa^a, M. Tosi^{a,b}, M. Zanetti, P. Zotto^{a,b}, A. Zucchetta^{a,b,2}, G. Zumerle^{a,b}

INFN Sezione di Pavia ^{a}, Università di Pavia ^{b}, Pavia, Italy

A. Braghieri^a, A. Magnani^a, P. Montagna^{a,b}, S.P. Ratti^{a,b}, V. Re^a, C. Riccardi^{a,b}, P. Salvini^a, I. Vai^a, P. Vitulo^{a,b}

INFN Sezione di Perugia ^{a}, Università di Perugia ^{b}, Perugia, Italy

L. Alunni Solestizi^{a,b}, G.M. Bilei^a, D. Ciangottini^{a,b,2}, L. Fanò^{a,b}, P. Lariccia^{a,b}, G. Mantovani^{a,b}, M. Menichelli^a, A. Saha^a, A. Santocchia^{a,b}

INFN Sezione di Pisa ^{a}, Università di Pisa ^{b}, Scuola Normale Superiore di Pisa ^{c}, Pisa, Italy

K. Androsov^{a,32}, P. Azzurri^{a,2}, G. Bagliesi^a, J. Bernardini^a, T. Boccali^a, R. Castaldi^a, M.A. Ciocci^{a,32}, R. Dell'Orso^a, S. Donato^{a,c,2}, G. Fedi, L. Foà^{a,c†}, A. Giassi^a, M.T. Grippo^{a,32}, F. Ligabue^{a,c}, T. Lomtadze^a, L. Martini^{a,b}, A. Messineo^{a,b}, F. Palla^a, A. Rizzi^{a,b}, A. Savoy-Navarro^{a,33}, A.T. Serban^a, P. Spagnolo^a, R. Tenchini^a, G. Tonelli^{a,b}, A. Venturi^a, P.G. Verdini^a

INFN Sezione di Roma ^{a}, Università di Roma ^{b}, Roma, Italy

L. Barone^{a,b}, F. Cavallari^a, G. D'imperio^{a,b,2}, D. Del Re^{a,b,2}, M. Diemoz^a, S. Gelli^{a,b}, C. Jorda^a, E. Longo^{a,b}, F. Margaroli^{a,b}, P. Meridiani^a, G. Organtini^{a,b}, R. Paramatti^a, F. Preiato^{a,b}, S. Rahatlou^{a,b}, C. Rovelli^a, F. Santanastasio^{a,b}, P. Traczyk^{a,b,2}

INFN Sezione di Torino ^{a}, Università di Torino ^{b}, Torino, Italy, Università del Piemonte Orientale ^{c}, Novara, Italy

N. Amapane^{a,b}, R. Arcidiacono^{a,c,2}, S. Argiro^{a,b}, M. Arneodo^{a,c}, R. Bellan^{a,b}, C. Biino^a, N. Cartiglia^a, M. Costa^{a,b}, R. Covarelli^{a,b}, A. Degano^{a,b}, N. Demaria^a, L. Finco^{a,b,2},

B. Kiani^{a,b}, C. Mariotti^a, S. Maselli^a, E. Migliore^{a,b}, V. Monaco^{a,b}, E. Monteil^{a,b}, M.M. Obertino^{a,b}, L. Pacher^{a,b}, N. Pastrone^a, M. Pelliccioni^a, G.L. Pinna Angioni^{a,b}, F. Ravera^{a,b}, A. Romero^{a,b}, M. Ruspa^{a,c}, R. Sacchi^{a,b}, A. Solano^{a,b}, A. Staiano^a

INFN Sezione di Trieste ^{a}, Università di Trieste ^{b}, Trieste, Italy
S. Belforte^a, V. Candelise^{a,b,2}, M. Casarsa^a, F. Cossutti^a, G. Della Ricca^{a,b}, B. Gobbo^a, C. La Licata^{a,b}, M. Marone^{a,b}, A. Schizzi^{a,b}, A. Zanetti^a

Kangwon National University, Chunchon, Korea
A. Kropivnitskaya, S.K. Nam

Kyungpook National University, Daegu, Korea
D.H. Kim, G.N. Kim, M.S. Kim, D.J. Kong, S. Lee, Y.D. Oh, A. Sakharov, D.C. Son

Chonbuk National University, Jeonju, Korea
J.A. Brochero Cifuentes, H. Kim, T.J. Kim

Chonnam National University, Institute for Universe and Elementary Particles, Kwangju, Korea
S. Song

Korea University, Seoul, Korea
S. Choi, Y. Go, D. Gyun, B. Hong, H. Kim, Y. Kim, B. Lee, K. Lee, K.S. Lee, S. Lee, S.K. Park, Y. Roh

Seoul National University, Seoul, Korea
H.D. Yoo

University of Seoul, Seoul, Korea
M. Choi, H. Kim, J.H. Kim, J.S.H. Lee, I.C. Park, G. Ryu, M.S. Ryu

Sungkyunkwan University, Suwon, Korea
Y. Choi, J. Goh, D. Kim, E. Kwon, J. Lee, I. Yu

Vilnius University, Vilnius, Lithuania
V. Dudenas, A. Juodagalvis, J. Vaitkus

National Centre for Particle Physics, Universiti Malaya, Kuala Lumpur, Malaysia
I. Ahmed, Z.A. Ibrahim, J.R. Komaragiri, M.A.B. Md Ali[34], F. Mohamad Idris[35], W.A.T. Wan Abdullah, M.N. Yusli

Centro de Investigacion y de Estudios Avanzados del IPN, Mexico City, Mexico
E. Casimiro Linares, H. Castilla-Valdez, E. De La Cruz-Burelo, I. Heredia-De La Cruz[36], A. Hernandez-Almada, R. Lopez-Fernandez, A. Sanchez-Hernandez

Universidad Iberoamericana, Mexico City, Mexico
S. Carrillo Moreno, F. Vazquez Valencia

Benemerita Universidad Autonoma de Puebla, Puebla, Mexico
I. Pedraza, H.A. Salazar Ibarguen

Universidad Autónoma de San Luis Potosí, San Luis Potosí, Mexico

A. Morelos Pineda

University of Auckland, Auckland, New Zealand

D. Krofcheck

University of Canterbury, Christchurch, New Zealand

P.H. Butler

National Centre for Physics, Quaid-I-Azam University, Islamabad, Pakistan

A. Ahmad, M. Ahmad, Q. Hassan, H.R. Hoorani, W.A. Khan, T. Khurshid, M. Shoaib

National Centre for Nuclear Research, Swierk, Poland

H. Bialkowska, M. Bluj, B. Boimska, T. Frueboes, M. Górski, M. Kazana, K. Nawrocki, K. Romanowska-Rybinska, M. Szleper, P. Zalewski

Institute of Experimental Physics, Faculty of Physics, University of Warsaw, Warsaw, Poland

G. Brona, K. Bunkowski, A. Byszuk[37], K. Doroba, A. Kalinowski, M. Konecki, J. Krolikowski, M. Misiura, M. Olszewski, M. Walczak

Laboratório de Instrumentação e Física Experimental de Partículas, Lisboa, Portugal

P. Bargassa, C. Beirão Da Cruz E Silva, A. Di Francesco, P. Faccioli, P.G. Ferreira Parracho, M. Gallinaro, N. Leonardo, L. Lloret Iglesias, F. Nguyen, J. Rodrigues Antunes, J. Seixas, O. Toldaiev, D. Vadruccio, J. Varela, P. Vischia

Joint Institute for Nuclear Research, Dubna, Russia

S. Afanasiev, P. Bunin, M. Gavrilenko, I. Golutvin, I. Gorbunov, A. Kamenev, V. Karjavin, V. Konoplyanikov, A. Lanev, A. Malakhov, V. Matveev[38,39], P. Moisenz, V. Palichik, V. Perelygin, S. Shmatov, S. Shulha, N. Skatchkov, V. Smirnov, A. Zarubin

Petersburg Nuclear Physics Institute, Gatchina (St. Petersburg), Russia

V. Golovtsov, Y. Ivanov, V. Kim[40], E. Kuznetsova, P. Levchenko, V. Murzin, V. Oreshkin, I. Smirnov, V. Sulimov, L. Uvarov, S. Vavilov, A. Vorobyev

Institute for Nuclear Research, Moscow, Russia

Yu. Andreev, A. Dermenev, S. Gninenko, N. Golubev, A. Karneyeu, M. Kirsanov, N. Krasnikov, A. Pashenkov, D. Tlisov, A. Toropin

Institute for Theoretical and Experimental Physics, Moscow, Russia

V. Epshteyn, V. Gavrilov, N. Lychkovskaya, V. Popov, I. Pozdnyakov, G. Safronov, A. Spiridonov, E. Vlasov, A. Zhokin

National Research Nuclear University 'Moscow Engineering Physics Institute' (MEPhI), Moscow, Russia

A. Bylinkin

P.N. Lebedev Physical Institute, Moscow, Russia

V. Andreev, M. Azarkin[39], I. Dremin[39], M. Kirakosyan, A. Leonidov[39], G. Mesyats, S.V. Rusakov

Skobeltsyn Institute of Nuclear Physics, Lomonosov Moscow State University, Moscow, Russia

A. Baskakov, A. Belyaev, E. Boos, V. Bunichev, M. Dubinin[41], L. Dudko, A. Ershov, V. Klyukhin, O. Kodolova, N. Korneeva, I. Lokhtin, I. Myagkov, S. Obraztsov, M. Perfilov, V. Savrin

State Research Center of Russian Federation, Institute for High Energy Physics, Protvino, Russia

I. Azhgirey, I. Bayshev, S. Bitioukov, V. Kachanov, A. Kalinin, D. Konstantinov, V. Krychkine, V. Petrov, R. Ryutin, A. Sobol, L. Tourtchanovitch, S. Troshin, N. Tyurin, A. Uzunian, A. Volkov

University of Belgrade, Faculty of Physics and Vinca Institute of Nuclear Sciences, Belgrade, Serbia

P. Adzic[42], P. Cirkovic, J. Milosevic, V. Rekovic

Centro de Investigaciones Energéticas Medioambientales y Tecnológicas (CIEMAT), Madrid, Spain

J. Alcaraz Maestre, E. Calvo, M. Cerrada, M. Chamizo Llatas, N. Colino, B. De La Cruz, A. Delgado Peris, D. Domínguez Vázquez, A. Escalante Del Valle, C. Fernandez Bedoya, J.P. Fernández Ramos, J. Flix, M.C. Fouz, P. Garcia-Abia, O. Gonzalez Lopez, S. Goy Lopez, J.M. Hernandez, M.I. Josa, E. Navarro De Martino, A. Pérez-Calero Yzquierdo, J. Puerta Pelayo, A. Quintario Olmeda, I. Redondo, L. Romero, J. Santaolalla, M.S. Soares

Universidad Autónoma de Madrid, Madrid, Spain

C. Albajar, J.F. de Trocóniz, M. Missiroli, D. Moran

Universidad de Oviedo, Oviedo, Spain

J. Cuevas, J. Fernandez Menendez, S. Folgueras, I. Gonzalez Caballero, E. Palencia Cortezon, J.M. Vizan Garcia

Instituto de Física de Cantabria (IFCA), CSIC-Universidad de Cantabria, Santander, Spain

I.J. Cabrillo, A. Calderon, J.R. Castiñeiras De Saa, P. De Castro Manzano, M. Fernandez, J. Garcia-Ferrero, G. Gomez, A. Lopez Virto, J. Marco, R. Marco, C. Martinez Rivero, F. Matorras, J. Piedra Gomez, T. Rodrigo, A.Y. Rodríguez-Marrero, A. Ruiz-Jimeno, L. Scodellaro, N. Trevisani, I. Vila, R. Vilar Cortabitarte

CERN, European Organization for Nuclear Research, Geneva, Switzerland

D. Abbaneo, E. Auffray, G. Auzinger, M. Bachtis, P. Baillon, A.H. Ball, D. Barney, A. Benaglia, J. Bendavid, L. Benhabib, J.F. Benitez, G.M. Berruti, P. Bloch, A. Bocci, A. Bonato, C. Botta, H. Breuker, T. Camporesi, R. Castello, G. Cerminara, M. D'Alfonso, D. d'Enterria, A. Dabrowski, V. Daponte, A. David, M. De Gruttola, F. De Guio, A. De

Roeck, S. De Visscher, E. Di Marco[43], M. Dobson, M. Dordevic, B. Dorney, T. du Pree, D. Duggan, M. Dünser, N. Dupont, A. Elliott-Peisert, G. Franzoni, J. Fulcher, W. Funk, D. Gigi, K. Gill, D. Giordano, M. Girone, F. Glege, R. Guida, S. Gundacker, M. Guthoff, J. Hammer, P. Harris, J. Hegeman, V. Innocente, P. Janot, H. Kirschenmann, M.J. Kortelainen, K. Kousouris, K. Krajczar, P. Lecoq, C. Lourenço, M.T. Lucchini, N. Magini, L. Malgeri, M. Mannelli, A. Martelli, L. Masetti, F. Meijers, S. Mersi, E. Meschi, F. Moortgat, S. Morovic, M. Mulders, M.V. Nemallapudi, H. Neugebauer, S. Orfanelli[44], L. Orsini, L. Pape, E. Perez, M. Peruzzi, A. Petrilli, G. Petrucciani, A. Pfeiffer, D. Piparo, A. Racz, T. Reis, G. Rolandi[45], M. Rovere, M. Ruan, H. Sakulin, C. Schäfer, C. Schwick, M. Seidel, A. Sharma, P. Silva, M. Simon, P. Sphicas[46], J. Steggemann, B. Stieger, M. Stoye, Y. Takahashi, D. Treille, A. Triossi, A. Tsirou, G.I. Veres[23], N. Wardle, H.K. Wöhri, A. Zagozdzinska[37], W.D. Zeuner

Paul Scherrer Institut, Villigen, Switzerland

W. Bertl, K. Deiters, W. Erdmann, R. Horisberger, Q. Ingram, H.C. Kaestli, D. Kotlinski, U. Langenegger, D. Renker, T. Rohe

Institute for Particle Physics, ETH Zurich, Zurich, Switzerland

F. Bachmair, L. Bäni, L. Bianchini, B. Casal, G. Dissertori, M. Dittmar, M. Donegà, P. Eller, C. Grab, C. Heidegger, D. Hits, J. Hoss, G. Kasieczka, W. Lustermann, B. Mangano, M. Marionneau, P. Martinez Ruiz del Arbol, M. Masciovecchio, D. Meister, F. Micheli, P. Musella, F. Nessi-Tedaldi, F. Pandolfi, J. Pata, F. Pauss, L. Perrozzi, M. Quittnat, M. Rossini, A. Starodumov[47], M. Takahashi, V.R. Tavolaro, K. Theofilatos, R. Wallny

Universität Zürich, Zurich, Switzerland

T.K. Aarrestad, C. Amsler[48], L. Caminada, M.F. Canelli, V. Chiochia, A. De Cosa, C. Galloni, A. Hinzmann, T. Hreus, B. Kilminster, C. Lange, J. Ngadiuba, D. Pinna, P. Robmann, F.J. Ronga, D. Salerno, Y. Yang

National Central University, Chung-Li, Taiwan

M. Cardaci, K.H. Chen, T.H. Doan, Sh. Jain, R. Khurana, M. Konyushikhin, C.M. Kuo, W. Lin, Y.J. Lu, S.S. Yu

National Taiwan University (NTU), Taipei, Taiwan

Arun Kumar, R. Bartek, P. Chang, Y.H. Chang, Y.W. Chang, Y. Chao, K.F. Chen, P.H. Chen, C. Dietz, F. Fiori, U. Grundler, W.-S. Hou, Y. Hsiung, Y.F. Liu, R.-S. Lu, M. Miñano Moya, E. Petrakou, J.f. Tsai, Y.M. Tzeng

Chulalongkorn University, Faculty of Science, Department of Physics, Bangkok, Thailand

B. Asavapibhop, K. Kovitanggoon, G. Singh, N. Srimanobhas, N. Suwonjandee

Cukurova University, Adana, Turkey

A. Adiguzel, M.N. Bakirci[49], S. Cerci[50], Z.S. Demiroglu, C. Dozen, E. Eskut, S. Girgis, G. Gokbulut, Y. Guler, E. Gurpinar, I. Hos, E.E. Kangal[51], G. Onengut[52], K. Ozdemir[53], A. Polatoz, D. Sunar Cerci[50], H. Topakli[49], M. Vergili, C. Zorbilmez

Middle East Technical University, Physics Department, Ankara, Turkey
I.V. Akin, B. Bilin, S. Bilmis, B. Isildak[54], G. Karapinar[55], M. Yalvac, M. Zeyrek

Bogazici University, Istanbul, Turkey
E. Gülmez, M. Kaya[56], O. Kaya[57], E.A. Yetkin[58], T. Yetkin[59]

Istanbul Technical University, Istanbul, Turkey
A. Cakir, K. Cankocak, S. Sen[60], F.I. Vardarlı

Institute for Scintillation Materials of National Academy of Science of Ukraine, Kharkov, Ukraine
B. Grynyov

National Scientific Center, Kharkov Institute of Physics and Technology, Kharkov, Ukraine
L. Levchuk, P. Sorokin

University of Bristol, Bristol, United Kingdom
R. Aggleton, F. Ball, L. Beck, J.J. Brooke, E. Clement, D. Cussans, H. Flacher, J. Goldstein, M. Grimes, G.P. Heath, H.F. Heath, J. Jacob, L. Kreczko, C. Lucas, Z. Meng, D.M. Newbold[61], S. Paramesvaran, A. Poll, T. Sakuma, S. Seif El Nasr-storey, S. Senkin, D. Smith, V.J. Smith

Rutherford Appleton Laboratory, Didcot, United Kingdom
K.W. Bell, A. Belyaev[62], C. Brew, R.M. Brown, L. Calligaris, D. Cieri, D.J.A. Cockerill, J.A. Coughlan, K. Harder, S. Harper, E. Olaiya, D. Petyt, C.H. Shepherd-Themistocleous, A. Thea, I.R. Tomalin, T. Williams, S.D. Worm

Imperial College, London, United Kingdom
M. Baber, R. Bainbridge, O. Buchmuller, A. Bundock, D. Burton, S. Casasso, M. Citron, D. Colling, L. Corpe, N. Cripps, P. Dauncey, G. Davies, A. De Wit, M. Della Negra, P. Dunne, A. Elwood, W. Ferguson, D. Futyan, G. Hall, G. Iles, M. Kenzie, R. Lane, R. Lucas[61], L. Lyons, A.-M. Magnan, S. Malik, J. Nash, A. Nikitenko[47], J. Pela, M. Pesaresi, K. Petridis, D.M. Raymond, A. Richards, A. Rose, C. Seez, A. Tapper, K. Uchida, M. Vazquez Acosta[63], T. Virdee, S.C. Zenz

Brunel University, Uxbridge, United Kingdom
J.E. Cole, P.R. Hobson, A. Khan, P. Kyberd, D. Leggat, D. Leslie, I.D. Reid, P. Symonds, L. Teodorescu, M. Turner

Baylor University, Waco, U.S.A.
A. Borzou, K. Call, J. Dittmann, K. Hatakeyama, H. Liu, N. Pastika

The University of Alabama, Tuscaloosa, U.S.A.
O. Charaf, S.I. Cooper, C. Henderson, P. Rumerio

Boston University, Boston, U.S.A.
D. Arcaro, A. Avetisyan, T. Bose, C. Fantasia, D. Gastler, P. Lawson, D. Rankin, C. Richardson, J. Rohlf, J. St. John, L. Sulak, D. Zou

Brown University, Providence, U.S.A.

J. Alimena, E. Berry, S. Bhattacharya, D. Cutts, N. Dhingra, A. Ferapontov, A. Garabedian, J. Hakala, U. Heintz, E. Laird, G. Landsberg, Z. Mao, M. Narain, S. Piperov, S. Sagir, R. Syarif

University of California, Davis, Davis, U.S.A.

R. Breedon, G. Breto, M. Calderon De La Barca Sanchez, S. Chauhan, M. Chertok, J. Conway, R. Conway, P.T. Cox, R. Erbacher, M. Gardner, W. Ko, R. Lander, M. Mulhearn, D. Pellett, J. Pilot, F. Ricci-Tam, S. Shalhout, J. Smith, M. Squires, D. Stolp, M. Tripathi, S. Wilbur, R. Yohay

University of California, Los Angeles, U.S.A.

R. Cousins, P. Everaerts, C. Farrell, J. Hauser, M. Ignatenko, D. Saltzberg, E. Takasugi, V. Valuev, M. Weber

University of California, Riverside, Riverside, U.S.A.

K. Burt, R. Clare, J. Ellison, J.W. Gary, G. Hanson, J. Heilman, M. Ivova PANEVA, P. Jandir, E. Kennedy, F. Lacroix, O.R. Long, A. Luthra, M. Malberti, M. Olmedo Negrete, A. Shrinivas, H. Wei, S. Wimpenny, B. R. Yates

University of California, San Diego, La Jolla, U.S.A.

J.G. Branson, G.B. Cerati, S. Cittolin, R.T. D'Agnolo, M. Derdzinski, A. Holzner, R. Kelley, D. Klein, J. Letts, I. Macneill, D. Olivito, S. Padhi, M. Pieri, M. Sani, V. Sharma, S. Simon, M. Tadel, A. Vartak, S. Wasserbaech[64], C. Welke, F. Würthwein, A. Yagil, G. Zevi Della Porta

University of California, Santa Barbara, Santa Barbara, U.S.A.

J. Bradmiller-Feld, C. Campagnari, A. Dishaw, V. Dutta, K. Flowers, M. Franco Sevilla, P. Geffert, C. George, F. Golf, L. Gouskos, J. Gran, J. Incandela, N. Mccoll, S.D. Mullin, J. Richman, D. Stuart, I. Suarez, C. West, J. Yoo

California Institute of Technology, Pasadena, U.S.A.

D. Anderson, A. Apresyan, A. Bornheim, J. Bunn, Y. Chen, J. Duarte, A. Mott, H.B. Newman, C. Pena, M. Pierini, M. Spiropulu, J.R. Vlimant, S. Xie, R.Y. Zhu

Carnegie Mellon University, Pittsburgh, U.S.A.

M.B. Andrews, V. Azzolini, A. Calamba, B. Carlson, T. Ferguson, M. Paulini, J. Russ, M. Sun, H. Vogel, I. Vorobiev

University of Colorado Boulder, Boulder, U.S.A.

J.P. Cumalat, W.T. Ford, A. Gaz, F. Jensen, A. Johnson, M. Krohn, T. Mulholland, U. Nauenberg, K. Stenson, S.R. Wagner

Cornell University, Ithaca, U.S.A.

J. Alexander, A. Chatterjee, J. Chaves, J. Chu, S. Dittmer, N. Eggert, N. Mirman, G. Nicolas Kaufman, J.R. Patterson, A. Rinkevicius, A. Ryd, L. Skinnari, L. Soffi, W. Sun, S.M. Tan, W.D. Teo, J. Thom, J. Thompson, J. Tucker, Y. Weng, P. Wittich

Fermi National Accelerator Laboratory, Batavia, U.S.A.

S. Abdullin, M. Albrow, G. Apollinari, S. Banerjee, L.A.T. Bauerdick, A. Beretvas, J. Berryhill, P.C. Bhat, G. Bolla, K. Burkett, J.N. Butler, H.W.K. Cheung, F. Chlebana, S. Cihangir, V.D. Elvira, I. Fisk, J. Freeman, E. Gottschalk, L. Gray, D. Green, S. Grünendahl, O. Gutsche, J. Hanlon, D. Hare, R.M. Harris, S. Hasegawa, J. Hirschauer, Z. Hu, B. Jayatilaka, S. Jindariani, M. Johnson, U. Joshi, A.W. Jung, B. Klima, B. Kreis, S. Lammel, J. Linacre, D. Lincoln, R. Lipton, T. Liu, R. Lopes De Sá, J. Lykken, K. Maeshima, J.M. Marraffino, V.I. Martinez Outschoorn, S. Maruyama, D. Mason, P. McBride, P. Merkel, K. Mishra, S. Mrenna, S. Nahn, C. Newman-Holmes, V. O'Dell, K. Pedro, O. Prokofyev, G. Rakness, E. Sexton-Kennedy, A. Soha, W.J. Spalding, L. Spiegel, N. Strobbe, L. Taylor, S. Tkaczyk, N.V. Tran, L. Uplegger, E.W. Vaandering, C. Vernieri, M. Verzocchi, R. Vidal, H.A. Weber, A. Whitbeck

University of Florida, Gainesville, U.S.A.

D. Acosta, P. Avery, P. Bortignon, D. Bourilkov, A. Carnes, M. Carver, D. Curry, S. Das, R.D. Field, I.K. Furic, S.V. Gleyzer, J. Hugon, J. Konigsberg, A. Korytov, J.F. Low, P. Ma, K. Matchev, H. Mei, P. Milenovic[65], G. Mitselmakher, D. Rank, R. Rossin, L. Shchutska, M. Snowball, D. Sperka, N. Terentyev, L. Thomas, J. Wang, S. Wang, J. Yelton

Florida International University, Miami, U.S.A.

S. Hewamanage, S. Linn, P. Markowitz, G. Martinez, J.L. Rodriguez

Florida State University, Tallahassee, U.S.A.

A. Ackert, J.R. Adams, T. Adams, A. Askew, S. Bein, J. Bochenek, B. Diamond, J. Haas, S. Hagopian, V. Hagopian, K.F. Johnson, A. Khatiwada, H. Prosper, M. Weinberg

Florida Institute of Technology, Melbourne, U.S.A.

M.M. Baarmand, V. Bhopatkar, S. Colafranceschi[66], M. Hohlmann, H. Kalakhety, D. Noonan, T. Roy, F. Yumiceva

University of Illinois at Chicago (UIC), Chicago, U.S.A.

M.R. Adams, L. Apanasevich, D. Berry, R.R. Betts, I. Bucinskaite, R. Cavanaugh, O. Evdokimov, L. Gauthier, C.E. Gerber, D.J. Hofman, P. Kurt, C. O'Brien, I.D. Sandoval Gonzalez, C. Silkworth, P. Turner, N. Varelas, Z. Wu, M. Zakaria

The University of Iowa, Iowa City, U.S.A.

B. Bilki[67], W. Clarida, K. Dilsiz, S. Durgut, R.P. Gandrajula, M. Haytmyradov, V. Khristenko, J.-P. Merlo, H. Mermerkaya[68], A. Mestvirishvili, A. Moeller, J. Nachtman, H. Ogul, Y. Onel, F. Ozok[58], A. Penzo, C. Snyder, E. Tiras, J. Wetzel, K. Yi

Johns Hopkins University, Baltimore, U.S.A.

I. Anderson, B.A. Barnett, B. Blumenfeld, N. Eminizer, D. Fehling, L. Feng, A.V. Gritsan, P. Maksimovic, C. Martin, M. Osherson, J. Roskes, A. Sady, U. Sarica, M. Swartz, M. Xiao, Y. Xin, C. You

The University of Kansas, Lawrence, U.S.A.

P. Baringer, A. Bean, G. Benelli, C. Bruner, R.P. Kenny III, D. Majumder, M. Malek, M. Murray, S. Sanders, R. Stringer, Q. Wang

Kansas State University, Manhattan, U.S.A.

A. Ivanov, K. Kaadze, S. Khalil, M. Makouski, Y. Maravin, A. Mohammadi, L.K. Saini, N. Skhirtladze, S. Toda

Lawrence Livermore National Laboratory, Livermore, U.S.A.

D. Lange, F. Rebassoo, D. Wright

University of Maryland, College Park, U.S.A.

C. Anelli, A. Baden, O. Baron, A. Belloni, B. Calvert, S.C. Eno, C. Ferraioli, J.A. Gomez, N.J. Hadley, S. Jabeen, R.G. Kellogg, T. Kolberg, J. Kunkle, Y. Lu, A.C. Mignerey, Y.H. Shin, A. Skuja, M.B. Tonjes, S.C. Tonwar

Massachusetts Institute of Technology, Cambridge, U.S.A.

A. Apyan, R. Barbieri, A. Baty, K. Bierwagen, S. Brandt, W. Busza, I.A. Cali, Z. Demiragli, L. Di Matteo, G. Gomez Ceballos, M. Goncharov, D. Gulhan, Y. Iiyama, G.M. Innocenti, M. Klute, D. Kovalskyi, Y.S. Lai, Y.-J. Lee, A. Levin, P.D. Luckey, A.C. Marini, C. Mcginn, C. Mironov, S. Narayanan, X. Niu, C. Paus, D. Ralph, C. Roland, G. Roland, J. Salfeld-Nebgen, G.S.F. Stephans, K. Sumorok, M. Varma, D. Velicanu, J. Veverka, J. Wang, T.W. Wang, B. Wyslouch, M. Yang, V. Zhukova

University of Minnesota, Minneapolis, U.S.A.

B. Dahmes, A. Evans, A. Finkel, A. Gude, P. Hansen, S. Kalafut, S.C. Kao, K. Klapoetke, Y. Kubota, Z. Lesko, J. Mans, S. Nourbakhsh, N. Ruckstuhl, R. Rusack, N. Tambe, J. Turkewitz

University of Mississippi, Oxford, U.S.A.

J.G. Acosta, S. Oliveros

University of Nebraska-Lincoln, Lincoln, U.S.A.

E. Avdeeva, K. Bloom, S. Bose, D.R. Claes, A. Dominguez, C. Fangmeier, R. Gonzalez Suarez, R. Kamalieddin, J. Keller, D. Knowlton, I. Kravchenko, F. Meier, J. Monroy, F. Ratnikov, J.E. Siado, G.R. Snow

State University of New York at Buffalo, Buffalo, U.S.A.

M. Alyari, J. Dolen, J. George, A. Godshalk, C. Harrington, I. Iashvili, J. Kaisen, A. Kharchilava, A. Kumar, S. Rappoccio, B. Roozbahani

Northeastern University, Boston, U.S.A.

G. Alverson, E. Barberis, D. Baumgartel, M. Chasco, A. Hortiangtham, A. Massironi, D.M. Morse, D. Nash, T. Orimoto, R. Teixeira De Lima, D. Trocino, R.-J. Wang, D. Wood, J. Zhang

Northwestern University, Evanston, U.S.A.

K.A. Hahn, A. Kubik, N. Mucia, N. Odell, B. Pollack, A. Pozdnyakov, M. Schmitt, S. Stoynev, K. Sung, M. Trovato, M. Velasco

University of Notre Dame, Notre Dame, U.S.A.

A. Brinkerhoff, N. Dev, M. Hildreth, C. Jessop, D.J. Karmgard, N. Kellams, K. Lannon, N. Marinelli, F. Meng, C. Mueller, Y. Musienko[38], M. Planer, A. Reinsvold, R. Ruchti, G. Smith, S. Taroni, N. Valls, M. Wayne, M. Wolf, A. Woodard

The Ohio State University, Columbus, U.S.A.

L. Antonelli, J. Brinson, B. Bylsma, L.S. Durkin, S. Flowers, A. Hart, C. Hill, R. Hughes, W. Ji, K. Kotov, T.Y. Ling, B. Liu, W. Luo, D. Puigh, M. Rodenburg, B.L. Winer, H.W. Wulsin

Princeton University, Princeton, U.S.A.

O. Driga, P. Elmer, J. Hardenbrook, P. Hebda, S.A. Koay, P. Lujan, D. Marlow, T. Medvedeva, M. Mooney, J. Olsen, C. Palmer, P. Piroué, H. Saka, D. Stickland, C. Tully, A. Zuranski

University of Puerto Rico, Mayaguez, U.S.A.

S. Malik

Purdue University, West Lafayette, U.S.A.

V.E. Barnes, D. Benedetti, D. Bortoletto, L. Gutay, M.K. Jha, M. Jones, K. Jung, D.H. Miller, N. Neumeister, B.C. Radburn-Smith, X. Shi, I. Shipsey, D. Silvers, J. Sun, A. Svyatkovskiy, F. Wang, W. Xie, L. Xu

Purdue University Calumet, Hammond, U.S.A.

N. Parashar, J. Stupak

Rice University, Houston, U.S.A.

A. Adair, B. Akgun, Z. Chen, K.M. Ecklund, F.J.M. Geurts, M. Guilbaud, W. Li, B. Michlin, M. Northup, B.P. Padley, R. Redjimi, J. Roberts, J. Rorie, Z. Tu, J. Zabel

University of Rochester, Rochester, U.S.A.

B. Betchart, A. Bodek, P. de Barbaro, R. Demina, Y. Eshaq, T. Ferbel, M. Galanti, A. Garcia-Bellido, J. Han, A. Harel, O. Hindrichs, A. Khukhunaishvili, G. Petrillo, P. Tan, M. Verzetti

Rutgers, The State University of New Jersey, Piscataway, U.S.A.

S. Arora, A. Barker, J.P. Chou, C. Contreras-Campana, E. Contreras-Campana, D. Ferencek, Y. Gershtein, R. Gray, E. Halkiadakis, D. Hidas, E. Hughes, S. Kaplan, R. Kunnawalkam Elayavalli, A. Lath, K. Nash, S. Panwalkar, M. Park, S. Salur, S. Schnetzer, D. Sheffield, S. Somalwar, R. Stone, S. Thomas, P. Thomassen, M. Walker

University of Tennessee, Knoxville, U.S.A.

M. Foerster, G. Riley, K. Rose, S. Spanier, A. York

Texas A&M University, College Station, U.S.A.

O. Bouhali[69], A. Castaneda Hernandez[69], A. Celik, M. Dalchenko, M. De Mattia, A. Delgado, S. Dildick, R. Eusebi, J. Gilmore, T. Huang, T. Kamon[70], V. Krutelyov, R. Mueller, I. Osipenkov, Y. Pakhotin, R. Patel, A. Perloff, A. Rose, A. Safonov, A. Tatarinov, K.A. Ulmer[2]

Texas Tech University, Lubbock, U.S.A.

N. Akchurin, C. Cowden, J. Damgov, C. Dragoiu, P.R. Dudero, J. Faulkner, S. Kunori, K. Lamichhane, S.W. Lee, T. Libeiro, S. Undleeb, I. Volobouev

Vanderbilt University, Nashville, U.S.A.

E. Appelt, A.G. Delannoy, S. Greene, A. Gurrola, R. Janjam, W. Johns, C. Maguire, Y. Mao, A. Melo, H. Ni, P. Sheldon, B. Snook, S. Tuo, J. Velkovska, Q. Xu

University of Virginia, Charlottesville, U.S.A.

M.W. Arenton, B. Cox, B. Francis, J. Goodell, R. Hirosky, A. Ledovskoy, H. Li, C. Lin, C. Neu, T. Sinthuprasith, X. Sun, Y. Wang, E. Wolfe, J. Wood, F. Xia

Wayne State University, Detroit, U.S.A.

C. Clarke, R. Harr, P.E. Karchin, C. Kottachchi Kankanamge Don, P. Lamichhane, J. Sturdy

University of Wisconsin - Madison, Madison, WI, U.S.A.

D.A. Belknap, D. Carlsmith, M. Cepeda, S. Dasu, L. Dodd, S. Duric, B. Gomber, M. Grothe, R. Hall-Wilton, M. Herndon, A. Hervé, P. Klabbers, A. Lanaro, A. Levine, K. Long, R. Loveless, A. Mohapatra, I. Ojalvo, T. Perry, G.A. Pierro, G. Polese, T. Ruggles, T. Sarangi, A. Savin, A. Sharma, N. Smith, W.H. Smith, D. Taylor, N. Woods

22: Also at Institute of Nuclear Research ATOMKI, Debrecen, Hungary

23: Also at Eötvös Loránd University, Budapest, Hungary

24: Also at University of Debrecen, Debrecen, Hungary

25: Also at Wigner Research Centre for Physics, Budapest, Hungary

26: Also at University of Visva-Bharati, Santiniketan, India

27: Now at King Abdulaziz University, Jeddah, Saudi Arabia

28: Also at University of Ruhuna, Matara, Sri Lanka

29: Also at Isfahan University of Technology, Isfahan, Iran

30: Also at University of Tehran, Department of Engineering Science, Tehran, Iran

31: Also at Plasma Physics Research Center, Science and Research Branch, Islamic Azad University, Tehran, Iran

32: Also at Università degli Studi di Siena, Siena, Italy

33: Also at Purdue University, West Lafayette, U.S.A.

34: Also at International Islamic University of Malaysia, Kuala Lumpur, Malaysia

35: Also at Malaysian Nuclear Agency, MOSTI, Kajang, Malaysia

36: Also at Consejo Nacional de Ciencia y Tecnología, Mexico city, Mexico

37: Also at Warsaw University of Technology, Institute of Electronic Systems, Warsaw, Poland

38: Also at Institute for Nuclear Research, Moscow, Russia

39: Now at National Research Nuclear University 'Moscow Engineering Physics Institute' (MEPhI), Moscow, Russia

40: Also at St. Petersburg State Polytechnical University, St. Petersburg, Russia

41: Also at California Institute of Technology, Pasadena, U.S.A.

42: Also at Faculty of Physics, University of Belgrade, Belgrade, Serbia

43: Also at INFN Sezione di Roma; Università di Roma, Roma, Italy

44: Also at National Technical University of Athens, Athens, Greece

45: Also at Scuola Normale e Sezione dell'INFN, Pisa, Italy

46: Also at University of Athens, Athens, Greece

47: Also at Institute for Theoretical and Experimental Physics, Moscow, Russia

48: Also at Albert Einstein Center for Fundamental Physics, Bern, Switzerland

49: Also at Gaziosmanpasa University, Tokat, Turkey

50: Also at Adiyaman University, Adiyaman, Turkey

51: Also at Mersin University, Mersin, Turkey

52: Also at Cag University, Mersin, Turkey

53: Also at Piri Reis University, Istanbul, Turkey

54: Also at Ozyegin University, Istanbul, Turkey

55: Also at Izmir Institute of Technology, Izmir, Turkey

56: Also at Marmara University, Istanbul, Turkey

57: Also at Kafkas University, Kars, Turkey

58: Also at Mimar Sinan University, Istanbul, Istanbul, Turkey

59: Also at Yildiz Technical University, Istanbul, Turkey

60: Also at Hacettepe University, Ankara, Turkey

61: Also at Rutherford Appleton Laboratory, Didcot, United Kingdom

62: Also at School of Physics and Astronomy, University of Southampton, Southampton, United Kingdom

63: Also at Instituto de Astrofísica de Canarias, La Laguna, Spain

64: Also at Utah Valley University, Orem, U.S.A.

65: Also at University of Belgrade, Faculty of Physics and Vinca Institute of Nuclear Sciences, Belgrade, Serbia

66: Also at Facoltà Ingegneria, Università di Roma, Roma, Italy
67: Also at Argonne National Laboratory, Argonne, U.S.A.
68: Also at Erzincan University, Erzincan, Turkey
69: Also at Texas A&M University at Qatar, Doha, Qatar
70: Also at Kyungpook National University, Daegu, Korea